3D DIGITAL RELIEF GENERATION

MEILI WANG

July 2011

National Centre for Computer Animation

Bournemouth University

3D DIGITAL RELIEF GENERATION

MEILI WANG

A thesis submitted in partial fulfilment of the requirements of the Media School of Bournemouth University for the degree of Doctor of Philosophy

July 2011

National Centre for Computer Animation

Bournemouth University

ABSTRACT

This thesis investigates a framework for generating reliefs. Relief is a special kind of sculptured artwork consisting of shapes carved on a surface so as to stand out from the surrounding background. Traditional relief creation is done by hand and is therefore a laborious process. In addition, hand-made reliefs are hard to modify. Contrasted with this, digital relief can offer more flexibility as well as a less laborious alternative and can be easily adjusted.

This thesis reviews existing work and offers a framework to tackle the problem of generating three types of reliefs: bas reliefs, high reliefs and sunken reliefs. Considerably enhanced by incorporating gradient operations, an efficient bas relief generation method has been proposed, based on 2D images. An improvement of bas relief and high relief generation method based on 3D models has been provided as well, that employs mesh representation to process the model. This thesis is innovative in describing and evaluating sunken relief generation techniques. Two types of sunken reliefs have been generated: one is created with pure engraved lines, and the other is generated with smooth height transition between lines. The latter one is more complex to implement, and includes three elements: a line drawing image provides a input for contour lines; a rendered Lambertian image shares the same light direction of the relief and sets the visual cues and a depth image conveys the height information. These three elements have been combined to generate final sunken reliefs. It is the first time in computer graphics that a method for digital sunken relief generation has been proposed.

The main contribution of this thesis is to have proposed a systematic framework to generate all three types of reliefs. Results of this work can potentially provide references for craftsman, and this work could be beneficial for relief creation in the fields of both entertainment and manufacturing.

ACKNOWLEDGMENTS

LIST OF CONTENTS

LIST OF FIGURES

Abbreviations

Two Dimensional   2D

Three Dimensional   3D

Computer Aided Machinery   CAM

Shape from Shading   SfS

Partial Differential Equation   PDE

Adaptively Sampled Distance Fields   ADFs

High Dynamic Range   HDR

Unsharp Masking   USM

Scaling Factor   SF

CHAPTER 1

INTRODUCTION

1.1 Background

1.1.1 Sculpture

Sculpture is one of the most important art forms producing three dimensional (3D) representations of natural or imagined objects. It is also of significance in depicting a certain kind of symbolic view of objects and monuments.

Sculpture has a long history, which can be divided into the following: ancient sculpture, western sculpture from the Middle Ages to the seventeenth century, and modern sculpture (Causey 1998).

Sculpture has been developed since prehistoric times. Sculptures produced by ancient Egypt, for example, the Sphinx, the Palette of King Narmer etc. were more influenced by ritual significance than aesthetic considerations. In Europe,

there emerged a great number of religious architectural sculptures, for example, church buildings, especially cathedrals. Many renowned sculpture masters, such as Ghiberti, Donatello, the Della Robbia family etc. emerged during the highly formative Renaissance period. Recent development of sculpture has introduced different and complicated materials, textures, and techniques. Sculptors have also explored various and highly original applications of this special art form. Modern sculpture has incorporated light, sound, etc., which has made this art form even more interesting and attractive.

Sculpture is traditionally created by carving, welding, firing, moulding, casting or painting. There are varieties of materials for making sculpture, for example, marble, metal, glass, and wood, these materials are renowned for their enduring properties. Other materials, which are slightly less enduring, such as clay, textiles and softer metals, can also be used.

Figure 1. 1 Two views of a wooden statue of the Buddha from Chinese Song Dynasty, Museum of Shanghai (BattlestarVII 2011).

In general, sculpture can be classified into round sculpture and relief depending on the space occupied by this art form. Round sculpture is surrounded on all sides except the base. It is also known as sculpture "in the round", which means

it can be appreciated from any direction (as shown in Figure 1.1). In this way, different perception angle may deliver different information.

A relief sculpture spans two dimensional and three dimensional art forms. This form of sculpture differs from painting and drawing, which can only depict a virtual 3D image in 2D space. Contrasted with this, a 3D object can be represented immediately and vividly by relief sculpture. There are other differences between relief and other art forms: such as the method of production process, material used etc. The advantage of relief sculpture is that it takes up less than half of the space, while it still presents almost the same amount of detail that round sculpture does. Compared with drawings and paintings, relief sculpture portrays a vivid 3D object. It is a special and very distinct art form. More details are introduced in the following section.

1.1.2 Relief sculpture

Relief is a type of sculptured artwork which is carved on a plane or a surface unlike general free-standing sculptures (Flaxman 1829; Rogers 1974). The most distinguishing feature of reliefs compared with round sculptures is that they physically lie on some kind of background. There are three types of relief: high relief, (attached to a surface (Figure 1.2(a)), or free standing (Figure 1.2(b))), bas relief and sunken relief (as shown in Figure 1.2(c) and Figure 1.2(d)).

In high relief (alto relievo), the forms have over half of their natural depth attaching to a surface or separating from it; and in bas relief (basso relievo, low relief), the forms have under half of their natural depth always attaching to a surface. A piece of bas relief is suitable for scenes with several objects, landscape elements or architectures. In sunken relief, also known as intaglio or hollow relief, the objects are carved into a flat surface (Rogers 1974).

3

(a) High relief-attached to a surface

(British Museum 2009a).

(b) High relief- free standing

(British Museum 2009b).

(c) Bas relief (British Museum 2009a).

(d) Sunken relief (Gorbis Images 2009).

Figure 1. 2 Three types of relief.

Nowadays, reliefs have an enormous number of applications ranging from aesthetic perspective to practical use. Pseudo-reliefs, also known as relief-style images generated by computer can be used to design webpage logos, cartoon figures and packaging etc. Real carving relief or Computer Aided Machinery (CAM) generated relief can be represented as single pieces of artwork or be used as decorations to adorn the surfaces of furniture, walls, and a vast range of other items.

1.2 Motivations

Reliefs modify the actual form of a surface, causing it either to protrude or to be carved, whereas in a picture it is only the colour or texture of a surface that is modified, not its actual form. Reliefs occupy a whole range of intermediary position between the complete flatness of pictures and the full Three-Dimensionality of sculpture in the round. Although a relief art piece is a synthesis of 2D and 3D art forms, 3D forms cannot be easily translated into relief models in that relief generation may involve elements organization, spatial composition etc. To some extent, relief artists should acquire to combine the qualities of both the pictorial arts and the sculptural arts in their work. There are two aspects: one relates to pictorial matters such as pattern, linear design, composition and the use of perspective; the other aspect concerns direct sculptural matters such as the actual projection of the relief, and the volume and other 3D qualities of its forms (Rogers 1974).

Traditionally, relief creation by hand involves cumbersome and time-consuming work that requires both professional skills and artistic expertise. For example, the relief sculpture known as the Giant Relief (owned by the Ritz Hotel in London) was carved out of stone in the following stages (Nicknorris 2009): breaking down the stone into main planes or areas, drilling the surface to various desired depths and moving the unwanted material, rounding the main forms, designing the hair and facial features (if any), removing tool marks with flat chisels, improving hair and muscular definition (if any) and finally meticulously finishing all surfaces. The Giant Relief project began in late October 1998 and was completed by April 1999, taking nearly half a year.

Recently, computers have been adopted to assist relief generation. Image processing tools, such as Photoshop, Coly Photo Viewer, and CorelDraw can generate a relief-style image via digital image processing on pixels. However,

as a standard built-in function in these packages, such a method provides images which may not correspond to the actual required depth information of a relief. Their output is moreover of little use in actual manufacturing. CAM has been developed recently; such created reliefs can be of direct use in such fields as creation of medals, decorations etc. Furthermore, it is appealing that a digital relief enables creation of real relief products in a massive scale when it is used as input for the CAM system. However, CAM relief generation is based on geometry modelling which is tedious and requires considerable expertise. More directly, one can model a piece of relief by manipulating a 3D mesh using modelling software, such as 3DS max, Maya, Zbrush etc. However, it requires users to master the skills and start from scratch, both of those necessities being time-consuming and laborious.

This thesis intends to develop high relief, bas relief and sunken relief generation techniques, which can be encapsulated under a framework of digital relief generation. Each type of relief has its own style, as a fact of that, appropriate methods or techniques have to be designed to generate a particular type of relief. For example, to generate a bas relief requires presenting an object in a nearly flattened plane which requires preservation of details without distortion of shapes, so it is necessary to adopt non-linear compression methods when processing the data. A high relief allows its model to lift out of the surface to a certain height compared to a bas relief, therefore, it can relax the requirement of the non-linear compression and the method for high relief can use a relatively larger scale factor (compression ratio) than that for bas relief. A sunken relief is somehow similar to bas relief with a limited height but carving the object into a surface rather than lifting it out. It emphasizes the usage of lines to highlight the presence of complex features. Some bas relief generation techniques can be combined into sunken relief generation; however, additional methods are to be included to address the issues relating to lines and smooth shapes. The methods for different types of relief generation can be related to

one another and have cross over with one another although they are specially tailored to solve different problems.

1.3 Aims and objectives

The aim of this work is to develop a 3D digital relief generation framework taking images and meshes as input. The designed framework includes three techniques, which are able to generate bas relief, high relief and sunken relief.

The objectives of this thesis are to:

1. Review recent work on different techniques for generating reliefs and analyse their advantages and disadvantages.

2. Develop a method to generate bas reliefs based on a 2D image input.

3. Produce a method to create reliefs (bas reliefs and high reliefs) from a 3D mesh directly.

4. Design a method to produce sunken reliefs from a known 3D geometry.

1.4 Contributions

This thesis has developed three techniques to generate all three types of relief under a framework based on 2D image inputs and 3D mesh inputs. There are correlation and connection among these techniques, while these techniques are specially designed for different types of relief generation.

The contributions of this thesis are as follows.

1. A detailed review of work covering traditional relief generation techniques, recent research progress on computer-assisted relief generation, and existing digital relief generation techniques are discussed in this thesis.

2. The thesis describes an image-based bas relief generation technique with gradient operation method which bridges the current gap between image processing tools and industrial design packages. The final output as geometric mesh enables artists or designers to add additional textures and materials for their relief design.

3. The thesis also describes a method to generate 3D reliefs (both high reliefs and bas reliefs) directly from 3D shapes, rather than processing range image data. This method consists of two key steps to flatten a given 3D shape without changing its topology whilst preserving its detail: mesh enhancement by 3D Unsharp Masking (USM) is firstly applied to emphasizing the contrast of displayed 3D scenes, and then a non-linear scaling scheme is developed to achieve the final relief.

4. Two types of techniques for sunken relief generation, one with pure engraved lines, and the other incorporating the contour lines seamlessly with the smooth surfaces, are proposed. The latter one combines a line drawing image, a rendered image, and a depth image from 3D shapes to handle advanced sunken relief generation. This is the first attempt to implement a method designed for sunken relief generation.

1.5 Publications

During the period of the research, parts of this work have respectively been accepted or published at three international conferences. Moreover, one paper has been submitted to the journal *The Visual Computer*. They are listed as follows.

M., Wang, J., Chang, J., Pan, Jian J. Zhang. Image-based bas relief generation with gradient operation. Proceedings of the 11th IASTED International Conference Computer Graphics and Imaging February 17-19, 2010 Innsbruck, Austria.

M., Wang, J., Chang, Jian J. Zhang. A Review of Digital Relief Generation Techniques. The 2nd International Conference on Computer Engineering and Technology , April 16 - 18, 2010, Chengdu, China.

M., Wang, J., Kerber, J., Chang, Jian J. Zhang. Relief stylization from 3D models using featured lines. 27th Spring conference on Computer Graphics. April 28-30, 2011, Bratislava, Slovakia.

M., Wang, J., Chang, J., Kerber, Jian J. Zhang. A Framework for Digital Sunken Relief Generation Based on 3D Geometric Models. (Submitted to The Visual Computer).

1.6 Thesis outline

Chapter 1 provides a brief introduction of this thesis describing the research motivation and exploring the research objectives, contributions etc.

Chapter 2 reviews the development of digital relief generation over recent years. Relief generation techniques are classified into three types: image-based techniques, direct modelling techniques, and 3D model-based techniques. At the end of chapter's conclusion, evaluations and comparisons have been discussed.

Chapter 3 presents a bas relief generation algorithm based on a 2D image input with gradient operations, such as magnitude attenuation and image enhancement. These gradient operations can highly improve the quality of the

generated relief. This chapter also demonstrates the according results in detail, and compares with other methods.

Chapter 4 introduces a method of generating 3D reliefs from 3D shapes directly and details the results. Unlike previous research work, instead of processing range image data with image processing methods, the key task is to scale 3D meshes directly whilst keeping the maximum amount of detail to produce the visually appropriate features to reliefs.

Chapter 5 describes the techniques to produce two types of sunken reliefs from a known 3D geometry. One is to create relief works with pure engraved lines, whilst the other aims to create sunken reliefs by incorporating the contour lines seamlessly with the smooth surfaces. For the latter method, a line drawing image, a rendered Lambertian image and a depth image have been integrated to generate the advanced sunken relief.

Chapter 6 concludes this thesis, and analyses its limitations and proposes the potential directions for future research and development.

CHAPTER 2

RELATED WORK

2.1 Overview

This chapter details the development of digital relief generation over recent years. Relief generation techniques can be classified into three categories: image-based techniques, direct modelling techniques and 3D model-based techniques. This systematic review has the potential to provide valuable insights into the theory behind different concepts and options concerning a practical application. In addition, it could assist artists and designers to develop an in-depth understanding of current state of art techniques in relief generation.

2.2 Image-based relief generation

2.2.1 Bas relief generation by image processing

Initially, generating digital relief is intended to create relief-style images (fake reliefs) rather than models with depth information encoded. The underlying concept in generating bas-relief-style images is based on computing the difference between every pixel and its neighbours, which generates the relief (depth effect) by fading the similar colour of pixels and emphasizing different colour of pixels.
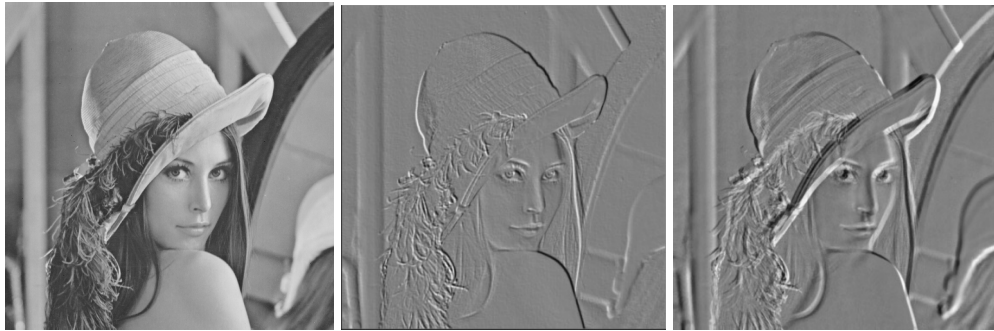
(a) Lena.
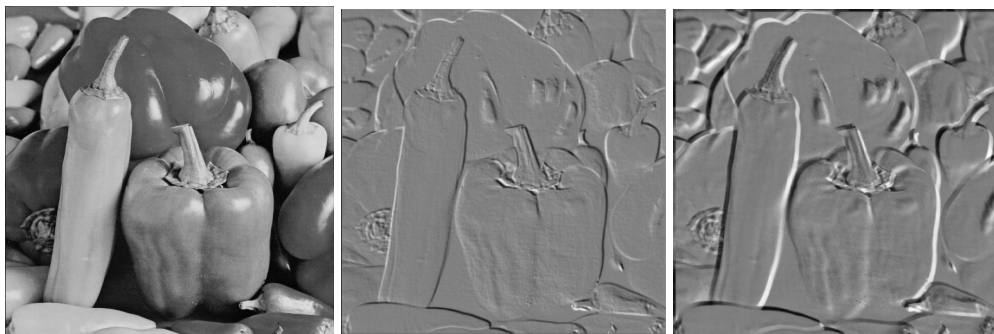
Pepper.

Figure 2. 1 Bas reliefs produced by Photoshop with different parameters (Photoshop 2009).

Such image processing techniques have been well developed and integrated into software such as Photoshop. Photoshop possesses bas relief (emboss) filter

that produces a relief-style image appearing to be slightly raised off or sunk into a surface. Also, users can set up optional angles and depths (the amount of the pixel difference). Furthermore, Photoshop establishes a subset of contour lines in the slope and relief operation to generate more realistic pseudo 3D effects. Figure 2.1 shows some examples of bas relief images produced by Photoshop (2009). Software such as Coly Photo Viewer and CorelDraw can also generate relief-style images that Photoshop does.

Producing natural relief-style images involves digital image processing, such as edge detection, image enhancement, filter, fusion etc. (Durand and Dorsey 2002; Paris and Durand 2006; Weiss 2006). Edge detection is one of the fundamental issues of digital image processing and computer vision. Edge detection algorithms can be classified as gradient-based edge detection and Laplacian-based edge detection. Sobel Operator, Robert's cross operator, Prewitt's operator, Laplacian of Gaussian and Canny edge detection algorithm are the most representative ones. For more details, please refer to Maini and Aggarwal (2009). Image enhancement aims to improve the perception information of images for human beings; especially it can be used as pre-processing tools for other image processing techniques to provide a more suitable input than the original image for a specific application. Image enhancement techniques can be divided into two broad categories: Spatial domain methods and frequency domain methods. The former operate directly on pixels, the latter operate on the Fourier transform of an image. Edge detection and image enhancement can be used as pre-processing methods by emphazing the most important features of images, therefore generating more convincing relief-style.

Similar relief generation techniques have been adopted to generate 2D animations with relief effects (Flash 2009). This technique is popular and widely used in webpage and advertisement design (China Visual 2009).

13

Other software, such as ArtCAM, Type3, JDPaint etc. provide functions for the design of 3D bas reliefs from single images. The idea is to generate reliefs by corresponding colour values to the height information. This process is easy to operate but the result may fail to meet the expectations (as indicated in Figure 2.2, the created relief includes many details and noise, such as the fur). Therefore, post-editing is required to achieve the desired result, which can be tedious.

2.2.2 Techniques relating to texture mapping

Bump mapping (FreeSpace 2009; Rogers and Earnshaw 1990) or roughness mapping can generate relief-style images as well by taking an image as a texture map. The result of bump mapping is still pseudo-reliefs because bump mapping modifies the surface normal only rather than the real depth/height data. It was claimed that Blinn (1978) firstly introduced bump mapping to make a surface appear rough. Bump mapping also closely relates to texture mapping (Heckbert 1986). Later, Peercy et al. (1997) improved bump mapping and pre-computed a texture of the disturbed normal in the tangent space. Their methods illustrated a more significant saving in hardware and rendering time than a straightforward implementation of bump mapping. Figure 2.3 presents an example of bump mapping.
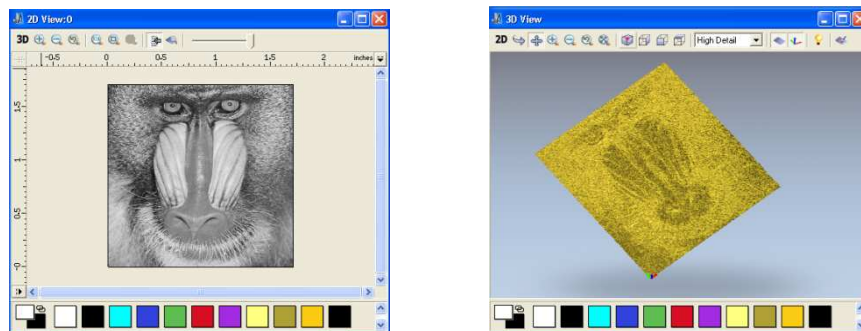
Figure 2. 2 ArtCAM failed to generate the relief from the image with complex colour distribution (ArtCAM 2009).

Displacement mapping (Hirche et al. 2004; Wang et al. 2004; Donnelly 2005) has been proposed, which provides an alternative technique for bump mapping. In displacement mapping, the surface is actually modified (for each point on a surface) compared with bump mapping where only the surface normal is modified. This means that the normal alone is disturbed in bump mapping but the geometry has been changed in displacement mapping. As a natural outcome therefore, displacement mapping can also generate relief-style images, but lead to deformation of the initial mesh to some extent.

(a) Diffuse texture.   (b) Normal map.   (c) Bump mapping result.

Figure 2. 3 Bump mapping result (Pudn 2009).

2.2.3 Shape from Shading

Shape from Shading (SfS), an approach to reconstructing the original 3D shape from a single image has proved a challenging task (Zeng et al. 2005; Agrawal et al. 2006; Prados and Faugeras 2005). In the 1980's, Horn and Brooks (1986) were the first to formulate the SfS problem simply and rigorously as that of finding the solution of a non-linear first-order Partial Differential Equation (PDE). Agrawal et al. (2006) proposed a generalized equation to represent a continuum of surface reconstruction using solutions of a given non-integrable gradient field.

Traditional SfS is not sufficient for relief generation without user intervention. One problem is bas relief ambiguity. Such ambiguity lies in the fact that the

reconstructed surface shape is not unique for a certain image under different lighting conditions (Belhumeur et al. (1999)). In some cases, researchers have to resort to human observation and knowledge to guide the generation of a suitable surface. To overcome the ambiguity, additional information is required and some assumptions have to be made to provide visual cues (Zeng et al. 2005).

Zeng et al. (2005) proposed an interactive approach that could efficiently resolve bas relief ambiguity. Their method requires users to set a reasonable surface normal first, SfS is then applied locally to the reconstruction of each surface patch and the local solutions are then combined to form a smooth global surface. Wu et al. (2008) presented another interactive system for reconstructing surface normals from a single image. They firstly improved the previous SfS algorithms to reconstruct a faithful normal for local image regions. Then they corrected low frequency errors using a simple mark up procedure. Their methods give rise to high-quality surfaces but require extensive user interaction (as shown in Figure 2.4). To sum up, SfS is an under-specified method requiring heavy user intervention when it has been applied to reconstructing certain surfaces.

Figure 2.4 demonstrates that SfS can be adopted for bas relief generation. However, there is an extensive requirement for user intervention. In the case of high relief, the effort rises drastically. Furthermore, there are further limitations as it only works for simple materials, but manifests problems when using colour images as inputs or those which contain complex textures. Moreover, the luminance entry in an image usually does not correspond to its geometric shape properties. For more details about SfS methods in general, please refer to Zhang et al. (1999).

(a)   (b)   (c)
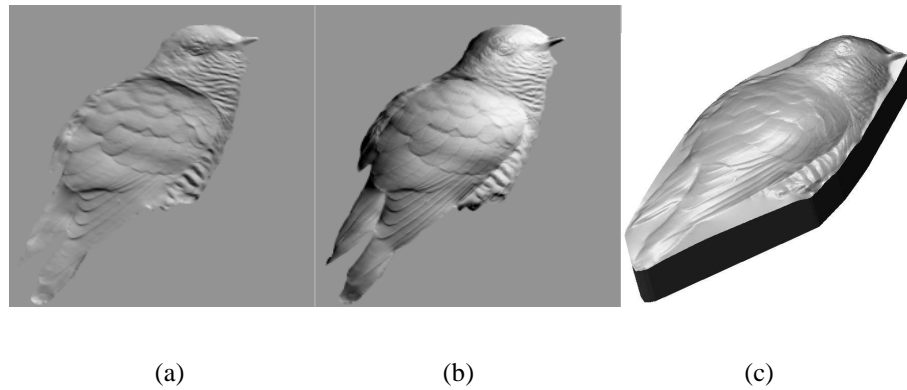
**Figure 2. 4 Normal map extracted by Wu et al. (2008). (a) A native Shape from
Shading approach. (b) Normal map after user editing. (c) The
reconstructed surface.**

Recently, Alexa and Matusik (2010) created reliefs whose appearance differs
when illuminated from different directional light sources instead of making
sure that an image looks faithful under one constant lighting condition. They
achieved this goal by placing small pyramids at the centre of each image pixel
and deforming them according to the desired reflectance properties. The
algorithm is capable of producing bas reliefs that contain information about a
pair of input images in one single piece of art. Moreover it can transfer the
colour information of a given image to the relief representation if directional
colour light sources are applied. This method is the first attempt to exploit the
nature of reliefs and their ambiguity and use them as a type of display.
However, it is hard to avoid a significant depth of the relief due to the large
difference in colour regions when working with colour images.

A different, but related, type of art known as Choshi is presented by Takayama
et al. (2010). An initial colour image was given, the image was first segmented
in partly constant patches, and then templates were produced to cut through
multiple colour layers and finally combined them together. The proposed
method can achieve a stylised but similar impression as long as the vantage
point is not changed significantly.

2.3 Relief generation by 3D design software or digital sculpture packages

Relief generation from images is often error-prone, as the colour or grey scale value of an image may not correspond to its geometric shape. Some digital image software can only generate pseudo 3D information that does not actually convey real height data. Shape from Shading aims at extracting the true geometric information, but it is reported that SfS cannot produce pleasant results without heavy user intervention.

Currently, 3D modelling software, such as 3DS MAX, Maya, Zbrush, Exchange 3D and Mudbox can model reliefs (both high reliefs and bas reliefs) by directly manipulating the true geometry as modelling other types of shapes. It is well known that such direct modelling is a tedious process and requires special skills and expertise. 3D modelling process is like real carving to some extent, with manipulation of vertices or control points replacing the cutting and shaping in the real world. They both need to create the object from scratch. However, the advantage of digital relief is that it can be easily modified, edited and stored. Figure 2.5 shows a lion head model as an example to demonstrate the result of direct modelling.
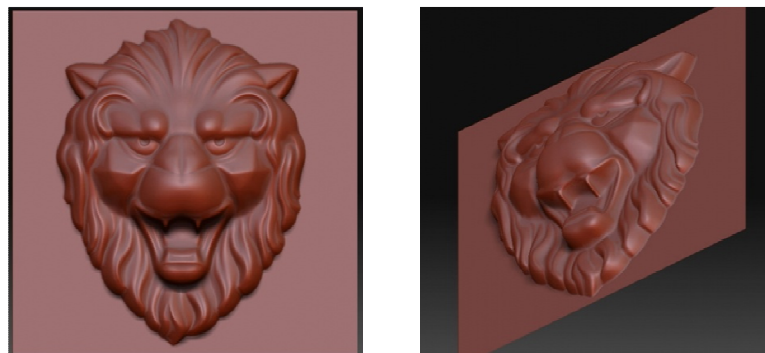
Figure 2. 5 A lion head modelled (Exchange3D 2009).

In contrast to 3D modelling software, Computer Aided Machinery software, such as ArtCAM, Type3, JDPaint etc. provide special tools which allow the user to design complicated relief models with different levels of control. Such designed relief can be machined into real relief by digital sculpting tools. It is nevertheless an elaborate procedure to generate high quality relief with complex details. Vector images can be used to design such reliefs instead of bitmap images. The vector images allow users to manipulate geometric primitives like points, lines, and curves based on mathematical equations to represent images in computer graphics (Orzan et al. 2008). In this way, the user can select the shapes from the templates, such as arch, pyramid and plane; the software then translates these template elements of a 2D vector image into –the 3D geometries (see Figure 2.6(a)). Figure 2.6(b) illustrates the original vector image and its final relief of a toy bear (ArtCAM 2009).

This kind of software is especially designed for art patterns with many useful templates for users to choose from. It saves an enormous amount of effort in modelling, yet has its limitations. Available shape templates may not be able to cover all kinds of extrusion, and furthermore, the creation of a vector image from scratch is a time-consuming process.

(a) ArtCAM shape templates.
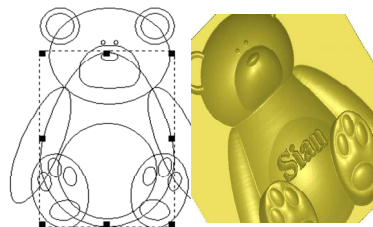
(b) A relief of teddy bear from a vector image using ArtCAM.

Figure 2. 6 The templates ArtCAM provided and an example (ArtCAM 2009).

Perry and Frisken (2001) developed a framework to generate sculpture digital characters by using digital clay named Kizamu. It is mainly based on Adaptively Sampled Distance Fields (ADFs) but Kizamu incorporates a blend of new algorithms representing significant technical advances in modelling. Their work is mainly addressed to users from the entertainment industry but, amongst others, the system allows creation of bas relief if a 3D model is given. To model the accurate behaviour of digital clay relies on the properties of ADFs and creative input. During the creative pipeline phase, the system offers different editing operations and tools to directly influence the outcome.

However, Sourin (2001a, 2001b) has also developed methods which provided an interactive system to directly produce a surface using programmed functions to represent shapes and manipulations. The surface and the tools are represented as functions that allow the computing of interplay efficiently.

The drawback of 3D modelling software or sculpture packages mentioned in this section is that the entire production process is time-consuming and needs close user intervention. The outcomes heavily depend on the skills and experience of the artist. The advantage over manual crafting is that the virtual tools allow editing, modifying, and storing the generated digital relief; furthermore, it is easy to reuse intermediate results or replicate the outcomes.

2.4 Relief generated from 3D shapes

Several essential fundamentals in model-based relief generation techniques and concepts require to be mentioned from the outset. They are height fields, tone mapping, Unsharp Masking (USM) and compression.

Height fields - The input to all methods presented in this section is a height field, also called range image or depth map. It encodes shapes by distance

information based on a regular 2D grid. Height fields can be achieved by either rendering a scene and reading the entries of the depth buffer, or casting rays and measuring the distance to the first intersection with a surface.

Tone Mapping or High Dynamic Range (HDR) - The problem of transforming a shape into a more planar representation can be regarded as a geometric analogy to the task in High Dynamic Range imaging. In HDR, a very large luminance interval has to be compressed without compromising visually significant features like contrast and small details, this action is also known as tone mapping. For relief generation, this corresponds to squeezing the depth interval range of a height field and simultaneously preserving the perceptibility of ridges, valleys and high frequency structures on surfaces. Since image and shape features are each of a very different nature, a straightforward adaption of HDR methods is not possible; nevertheless, most algorithms presented in this section are inspired by solutions from HDR.

Unsharp Masking (USM) - It is a well-known feature enhancement technique in image processing, which aims to split a given signal into low frequency and high frequency. An input image is convolved with a low pass kernel resulting in a smooth version of the input image. Subtracting the smooth version from the original image leads to a high frequency image containing peaks at small scale detail level. Adding a multiple of high frequency image back to the smooth image leads to an emphasis of fine structures in the newly reassembled image.

Compression - A height field is given, the first approach to compress its depth interval size would be a uniform linear rescaling of all entries. This only works as long as the compression ratio is not high. As soon as a significant ratio is required, the visibility of fine features is lost to a considerable extent. For bas reliefs, where a compression to 2% and less is common, the basic linear

approach fails since apart from the contours and some extreme discontinuities on the surface everything appears to be flat. Non-linear scaling schemes have been considered and developed to preserve the fine details.

To evaluate the most successful high quality results, sharpness, richness of detail and accuracy should be taken into account.

Current research on generating reliefs from 3D models can be classified into two categories: one based on perception and projection, the other based on geometry processing.

Cignoni et al. (1997) developed a computer-assisted relief generating system which was regarded as the earliest technique known for generating 3D bas and high reliefs from 3D models. They applied a compression inversely proportional to the height value followed by a linear rescaling. This resulted in a higher compression for those scene elements which were far away from an observer and has less effect on the more salient parts. Two approaches: image-precision based on the use of the Z-buffer and object-precision based on a visible surface detection algorithm were proposed. In the final, a given scene was rendered with the near and far clipping planes chosen in such a way that they tightly enclosed the scene. Although this work introduced by Cignoni et al. (1997) is the very first in this field and their methods are very successful for high relief generation, in terms of the visibility of details, this method is little better than linear rescaling in the case of bas reliefs. The authors noted that such perspective foreshortening relatively enlarges edges on a surface, and so a significant amount of the depth range remained wasted if these regions were not specifically treated. This observation made a significant contribution to the following research in this field.

Belhumeur et al. (1999) investigated the ambiguity of bas relief generation with respect to surface reconstruction. They proved that there existed a structure transformation from a shape to a corresponding bas relief, so that the shading and shadowing in both cases are identical if the viewer's perspective changes slightly around an orthogonal view. However, if an optimum angle of view is exceeded, it can produce distortion and unnatural results. This approach therefore ultimately relies on human perception.

Instead of projecting a 3D shape to the viewing plane (for capturing a height field), Song et al. (2007) firstly described a method to generate bas reliefs from 3D shapes automatically. They addressed the problem as geometry processing compared to the HDR image compression problem widely studied in computer graphics. They represented the shape in appropriate differential coordinates, and then used similar saliency measure as Lee et al. (2005) illustrated in mesh saliency under a certain viewpoint and then described it in differential coordinates; they subsequently used USM to enhance the features followed by a rescaling. Given the new differential coordinates, they had to solve a diffusion equation in order to retrieve the shape information. They were the first to investigate the derivatives for bas relief generation in order to distinguish between large and small surface features. Nevertheless, on balance their methods in general appear slightly complicated and their results do not look lifelike enough to justify such effort and seem sometimes look even distorted and exaggerated.

Kerber et al. (2007, 2007) developed feature preserving algorithms for range image compression inspired by the work of Song et al. (2007). They adopted the idea as Lee et al. (2005) to process the geometry and operated in the gradient domain. They performed a thresholding to eliminate extraordinarily large gradients as they appear on silhouettes and along the boundary of occlusions. Unsharp Masking with a Gaussian filter was applied to enhancing

fine and visually important features contained in the high frequency of the partial derivatives. Given the manipulated gradients, a solution of a Partial Differential Equation, a linear rescaling and then recombined to get the depth compressed result. After such strengthening, the perceptibility of the result was preserved, even for high compression ratios, which lead to the final bas relief. This approach is demonstrably simple, fast and produces results of an enhanced quality.

Gaussian blurring in the Unsharp Masking process, as described above, leads to a smearing of features and causes false responses in the high frequency image. This results in slightly exaggerated reliefs because the peaks are further enhanced. This problem can be solved if a more elaborated filtering is applied. Weyrich et al. (2007) provided a semi-automatic tool that helped artists to create bas reliefs making use of a silhouette preserving diffusion filter. The proposed silhouette preserving diffusion filter ensured the sharpness of gradient discontinuities. It could be regarded as the current state of the art in model-based bas relief generation. Their approach adapted methods from tone-mapping literature which addressed the related problem of squeezing a high dynamic range image into a low dynamic range one. Their work presented a similar technique that operated in the gradient domain and adopted a logarithmic attenuation function to compress large gradients. The proposed multi scale approach enabled an artist to direct the relative importance of different frequency bands. This offers enhanced artistic freedom and allows suppression of noise. They also analysed the interplay between the material properties for bas reliefs and the compression ratio with respect to the perceptibility of features. To date, this approach produces the most successful high quality results in terms of sharpness, richness of detail and accuracy. However, the quality and flexibility of this method are attained at the cost of diminished user-friendly performance. It requires direct personal intervention, as there are many parameters to be configured. This can make the production

of satisfactory reliefs a very time-consuming process, unless an experienced computer-artist is involved. Their work could provide a platform to produce more artistic results but it also requires the user to occasionally refine meaningful weights by trial and error.

The subsequent work (Kerber et al. 2009) focused on simplicity and user-friendliness. They restricted themselves to a single scale approach for Unsharp Masking during which a bilateral filter was used to smooth the gradient signal. A bilateral filter is known for its edge preserving nature. When being applied to the gradient of a height field, it ensures sharpness of curvature extrema as they appear at ridges and valleys. This consequently marks an improvement to their earlier work and it appears to be a good compromise in comparison to the more complex filters used by Weyrich et al. (2007). Regarding the application aspect they demonstrated how to produce seamless reliefs when stitching together multiple height fields for example to generate a collage or a cubism-like piece of art. The small compromises in this approach lead to a noticeable reduction of user defined parameters and as a result are much simpler and faster without too much sacrifice the quality and feature variety in the outcome. Thus, the time required for generating a visually pleasant and faithful relief drops significantly.

Recently, Kerber (2010) further improved the ease of use and performance by adding a user interface and implementing the algorithm on graphics hardware. This resulted in a real time application. It even permitted generation of dynamic reliefs given an animated model. In addition to a gradient domain approach, they also described a variant which directly operated on the depth map. They split the signal into three different layers; a rough and piecewise constant base layer which describes the overall shape, followed by coarse and fine features on the surface. This range domain method produces reasonable

results for high reliefs but, unlike the gradient domain counterpart, it becomes less effective if the compression ratio is too high.

The above-mentioned algorithms by Song et al. (2009), Weyrich et al. (2007) and Kerber et al. (2007) can be regarded as geometric variants of the high dynamic range compression methods presented by Fattal et al. (2002) and Durand and Dorsey (2002). Unlike these methods, that manipulate the gradients of a given shape, the work by Sun et al. (2009) operated directly on the height field and used gradient information only as additional weights. It allowed users to distinguish features on multiple scales and relied on the concept of adaptive histogram equalization primarily used for contrast enhancement in images. The algorithm produces competitive results but the required the pre-processing phase is considerably time-consuming. The authors suggested multiple optimizations which could help to overcome this issue.

| (a) | (b) | (c) | (d) |
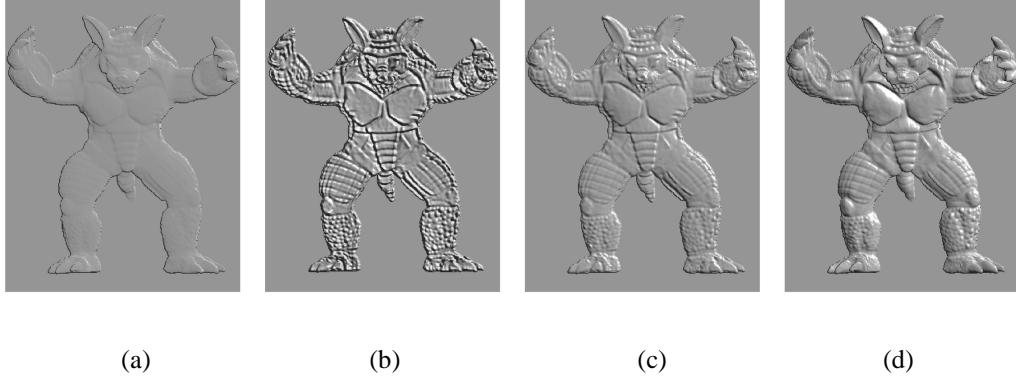
Figure 2. 7 Bas reliefs produced by (a) Cignoni et al. (1997). (b) Kerber et al. (2007b). (c) Kerber et al.(2009). (d) Sun et al.(2009).

These above-mentioned model-based bas relief generation techniques do not use exact mesh representation for bas relief generation. Figure 2.7 and Figure 2.8 present the compared results with different methods (Sun et al. (2009)). Figure 2.7(a) is the result attained through by a linear scaling after applying a compression inversely proportional to the height value; it can be readily seen

that the details are hardly preserved. Figure 2.7(c) greatly improves the previous result generated by Kerber et al. (2007) (Figure 2.7(b)) on generating vivid and natural relief models. Figure 2.7(d) provides the similar result to Figure 2.7(d), but looks more natural, generated by Sun et al. (2009) (Figure 2.7(d)).

Figure 2.8 shows bas reliefs of a building model. Figure 2.8 (a) shows larger height contrast in some details, e.g. the truck wheels generated by Sun et al. (2009) look sharper. Considering the stairs of the platform for instance, Figure 2.8(b) seems more natural.

(a)   (b)
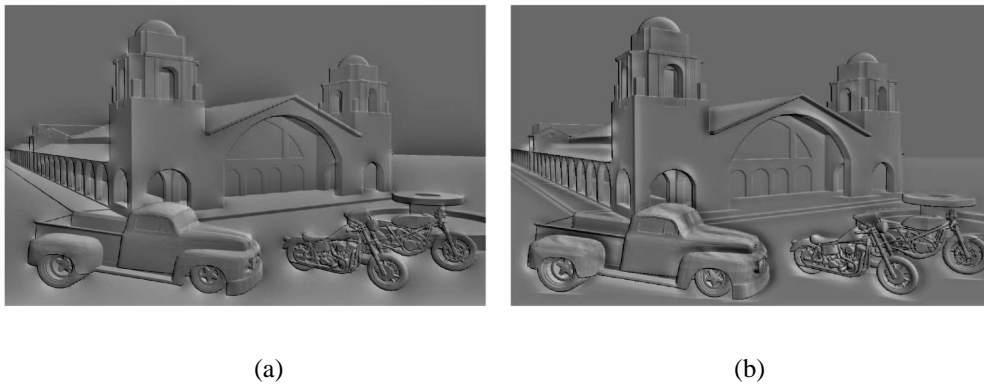
Figure 2. 8 (a) Bas relief of a building model produced by Weyrich et al. (2007). (b) Bas relief of the same scene produced by Sun et al. (2009).

2.5 Summary

In this chapter, the related research work on current digital relief generation techniques has been discussed. Relief generation from an image is the most mature technique to create relief-style images (only confined to bas reliefs) which could be used to design webpage logos, cartoon figures and packages, because such applications do not need actual height information; since it is important to recall that, it is easy to create relief-style images with tools such as

Photoshop. Other methods e.g. displacement mapping, Shape from Shading etc. are designed for specific alternation of the height information.

Reliefs generated from 3D shapes have been considered as a promising means to create both high reliefs and bas reliefs, and allow the reuse of existing 3D models of different objects. The final generated reliefs do convey real height information which could be easily machined directly into real reliefs in a CAM system. Moreover, the generated 3D relief can be edited and modified before machining.

CHAPTER 3

BAS RELIEF GENERATION BASED ON 2D IMAGES

3.1 Overview

A piece of bas relief is a synthesis of 2D and 3D art form. Bas relief can give the viewers a much stronger impression than ordinary images in that it conveys minor depth information. In this chapter, a novel method will be proposed to generate a piece of relief of a 3D mesh based on a 2D image input via gradient operations. The final output is a geometric mesh which enables artists or designers to add additional texture and material features for their relief design.

3.2 Background

Some image processing software, such as Photoshop, Coly Photo Viewer, and CorelDraw can generate a relief style image via direct operations on pixels. As a standard built-in function in those image processing packages, such a method provides a result that may not correspond to the required depth information of a relief. Their output is also of little use at the stage of actual manufacturing. With industrial design packages for bas relief generation, such as ArtCAM, Type3, JDPaint, the designed output can be machined into a real relief directly by engraving machines. However, special knowledge and professional skills are required to use such packages. The designing process can in consequence be tedious and time-consuming.

This chapter attempts to develop a method of building up a digital bas relief from a single image. This digitally generated bas relief will bridge the gap between image processing tools and industrial design packages. Its usage is envisaged as a tool for reconstruction of the existing reliefs or for fast generation of prototypes from images which can be further refined by designers using professional tools.

The proposed method occupies an intermediate position between image-based and model-based techniques. The main approach is introduced from 3D surface reconstruction (Zhang et al. 1999; Agrawal et al. 2006; Wu et al. 2008), but operates the image in its gradient domain to improve the quality of generated relief. The first step is to convert a given input image to grey scale one and treat the pixel values as entries of a height field. Then adopting similar technique introduced by Kerber et al. (2007), the proposed method produces a feature preserving 3D bas relief. Instead of a linear rescaling, the proposed method applies gamma correction to further equalise the visibility of features in areas of different depth levels.

3.3 Method description

This section describes the implementation of bas relief generation from an image. In practice, the pixel values can be used as the depth information (z-coordinate). However, a direct use without any processing of these pixel values does not produce the desired effects and may for example result in large shape distortion and feature blurring (As shown in Figure 2.9). Said et al. (2009) suggested opting out the factors affecting the resulting intensities, namely, surface colour, material properties, and light direction. In consequence, images with complex texture and background are not considered.

Briefly, the proposed method comprises the following operations:

1. inputting image data and converting to a grey level image with pixel value $I(x, y)$;
2. calculating image gradients $G = (G_x, G_y)$;
3. attenuating gradients to smooth the shape changes;
4. Unsharp Masking to boost the fine features;
5. constructing the modified image $I_r(x, y)$ by solving the Poisson equation to match the altered gradients;
6. applying gamma correction to achieve the final image $I_f(x, y)$;
7. transferring the final image $I_f(x, y)$ into a triangulated mesh representing the 3D relief shape.

These operations are executed in sequence as is outlined in Figure 3.1.
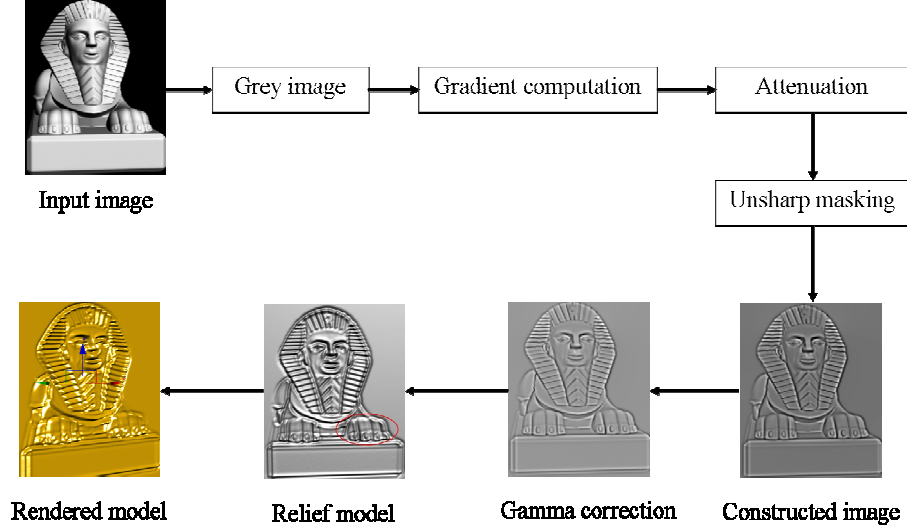
Figure 3. 1 Procedures of the proposed method.

3.3.1 Gradient computation

Image gradient is a directional change in the intensity or colour in an image. In implementation, gradient is the first order derivative of image pixel value $I(x, y)$ which is a vector combining members in x direction and in y direction. For each pixel, its value can be computed by forward difference as follows:

$$G_x = I(x+1, y) - I(x, y) \tag{3.1}$$

$$G_y = I(x, y+1) - I(x, y) \tag{3.2}$$

Figure 3.2 shows the gradient components in x and y direction.
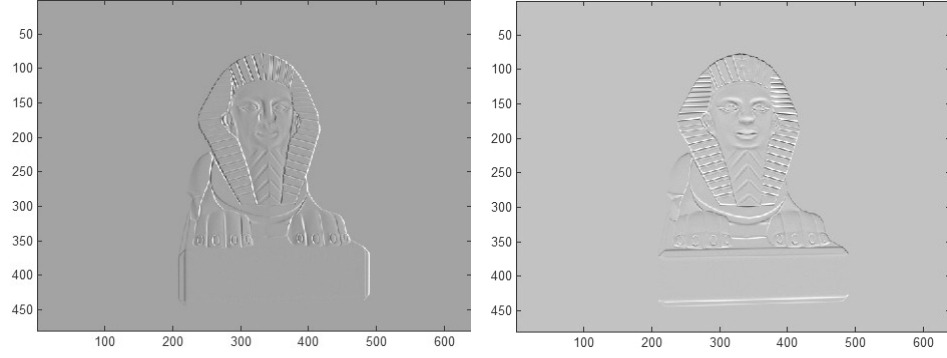
Figure 3. 2 Gradient components of the Sphinx model; x-component of gradient: G_x(left) and y-component of gradient: G_y(right).

3.3.2 Attenuation

Attenuation is an operation that reduces the values of larger magnitudes more significantly than those of the smaller ones do. Attenuation is useful for keeping the overall details of the image which are important regarding a major purpose of generating bas reliefs. Fattal et al. (2004) proposed the attenuation function in high dynamic range compression; this attenuation function can be adopted to achieve the gradient attenuation.

$$\overline{G}_x(x, y) = \frac{\alpha}{\|G_x(x, y)\|} \left(\frac{\|G_x(x, y)\|}{\alpha} \right)^{\beta} \tag{3.3}$$

$$\overline{G}_y(x, y) = \frac{\alpha}{\|G_y(x, y)\|} \left(\frac{\|G_y(x, y)\|}{\alpha} \right)^{\beta} \tag{3.4}$$

The first parameter α determines to what degree gradient magnitudes remain unchanged. Gradients of larger magnitude are attenuated (assuming $0 < \beta < 1$), while gradients of magnitude smaller than α are slightly magnified. Choosing $\alpha = 0.1$ and $\beta = 0.9$ works for bas relief generation as suggested by Fattal et al.

33

(2004). Figure 3.3 demonstrates the gradient images in *x* and *y* direction after attenuation.

Figure 3. 3 Updated x-component of gradient G$_x$ (left) and y-component of gradient G$_y$(right) after attenuation compared to Figure 3.2.

3.3.3 Boosting by Unsharp Masking

Attenuation alone is not sufficient for preserving fine details since the high frequency conveys small features. The high frequency information, that indicates the edges and fine features, should be boosted with Unsharp Masking in order to highlight them.

USM is a flexible and efficient method to enhance the perceptual quality of images containing depth information. The main principle is to subtract the created smoothed version from the original to obtain the high frequency part, which is then linearly scaled by a specified factor and added back to the original one (Luft et al. 2006; Badamchizadeh and Aghagolzadeh 2004).

In the gradient case:

$$\hat{G}_x = \overline{G}_x + \delta * (\overline{G}_x - blur(\overline{G}_x)) \tag{3.5}$$

$$\hat{G}_y = \overline{G}_y + \delta * (\overline{G}_y - blur(\overline{G}_y)) \tag{3.6}$$

34

In Equation 3.5 and 3.6, $blur(\overline{G}_x)$ stands for Gaussian smoothing (Kerber et al. 2007), δ is the amount of enhancement, and represents how much the high frequencies are boosted compared to the low frequencies. $\delta = 5$ is adopted according to the experiments. Figure 3.4 is the gradient images by USM.

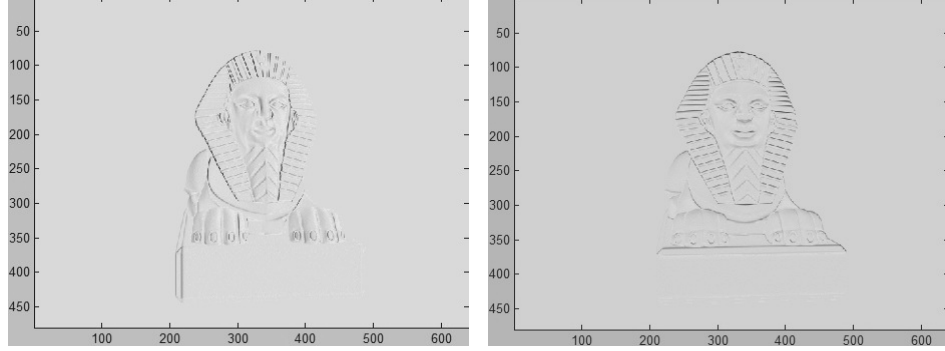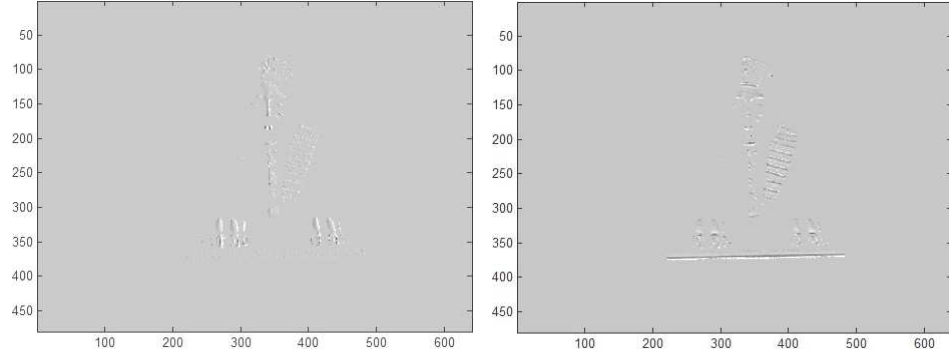**Figure 3. 4 Updated x-component of gradient G_x (left) and y-component of gradient G_y(right) after USM compared to Figure 3.3.**
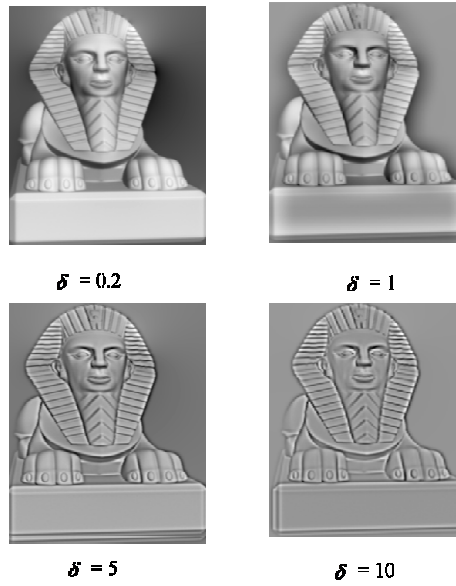
Figure 3. 5 Influence of different δ values.

Figure 3.5 shows the output image influenced by different δ from 0.2 to 10. The δ will influence the final relief models as well. The adjustment of δ could be useful of artistic control.

3.3.4 Image reconstruction from gradient field

According to the modified gradients from the above steps, the next task is to reconstruct the image $I_r(x, y)$ from the enhanced gradient $\hat{G}_x, \hat{G}_y$ by USM. Finding an approximate I_r, whose gradients are the closest to $\hat{G}$ is one of the solutions (Agrawal et al. 2006; P´erez et al. 2003). The solution of finding an approximate I_r is to derive the Poisson equation from the least square formulation.

$\arg \min_{I_r} \int \left\| \nabla I_r - \hat{G} \right\|^2$, which is equivalent to solving the Poisson equation:

$$\nabla^2 I_r - div(\hat{G}) = 0 \qquad (3.7)$$

Where $\nabla^2 = \dfrac{\partial}{\partial x^2} + \dfrac{\partial}{\partial y^2}$ denotes the Laplacian operator, and

$div(\hat{G}) = \dfrac{\partial \hat{G}_x}{\partial x} + \dfrac{\partial \hat{G}_y}{\partial y}$ stands for the divergence operator.

P´erez et al. (2003) introduced a technique to calculate the image pixel values, which required solving a sparse system of linear equations. It is straightforward to set the boundary values as the original pixel values to solve the linear equations.

3.3.5 Gamma correction

In order to get the result, the pixel values of an image must be compressed to serve the purpose of generating bas relief which implies that an image must be conformed to the depth degree of a bas relief. Generating the final bas relief requires normalizing the values of the recovery image to a range from 0 to 1.

Thereafter a correction step must be added to minimize possible distortion and deformation. One of the most popular approaches is gamma correction (Kim and MacDonald 2006), by a power function of gamma. Gamma correction affects the visual contrast, and a higher value indicates a higher level of contrast. The implementation of the normalised gamma correction is as follows:

$$I_f(x, y) = \left(\frac{I_r(x, y) - \min(I_r(x, y))}{\max(I_r(x, y))} \right)^{\frac{1}{g}} \tag{3.8}$$

Where g denotes the image gamma value. When $0 < g < 1$, gamma correction enhances contrast of bright regions, whereas when $g > 1$ it enhances contrast in dark regions. $g = 2.5$ is adopted to this model to achieve the highest contrasted images. Figure 3.6(a) shows the directly reconstructed image after solving the Possion equation without gamma correction and Figure 3.6(b) shows the reconstructed image after gamma correction and normalization. It can be observed that after gamma correction, the image is balanced with the nonlinear scale with its pixel values which therefore benefits the final 3D reconstruction.

(a) Image without gamma correction.   (b) Image after gamma correction.

Figure 3. 6 Gamma correction.

37

3.3.6 Mesh triangulation and simplification

After applying gamma correction, the mesh of a 3D bas relief can be generated. Triangular meshes have received wide acceptance as elementary representation for meshes and have been well studied (Owen 1998). The triangulated mesh is adopted to represent 3D relief models. For a simple implementation, pixel values $I_f(x, y)$ correspond to a depth z in Equation 3.8; accordingly, connectivities of 3D vertexes at each pixel constitute the triangular mesh. Figure 3.7 shows the reconstructed Sphinx model (left) and the enlarged claw of the Sphinx model (right). The claw is highlighted by the circle in Figure 3.7(a). The mesh simplification procedure (Cignoni 1998; Isenburg et al. 2003) can be applied to reducing the number of vertices whilst preserving the overall shape as much as possible. Other post-processing techniques, such as texturing and shading can be added to create further embellished results as shown in Figure 3.9. The mesh was rendered using Autodesk | Maya.

$$z = I_f(x, y) \qquad (3.9)$$
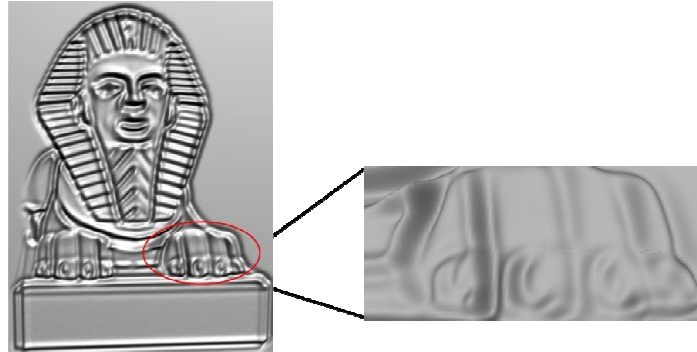
(a) The reconstructed Sphinx model.   (b) The reconstructed claw of the Sphinx model.

Figure 3. 7 The reconstructed Sphinx model and the claw of the Sphinx model.

3.4 Results and discussions

The proposed algorithm is straightforward to implement. A colour image is converted to a grey image, which is processed in the gradient domain as outlined in section 3.3. The depth of the bas relief can be user specified. The PC used is HP Workstation 4300, with Intel Pentium Dual CPU 3.2GHz and 2GB RAM, which is equipped with NVIDIA GeForce 7900 GTX video card. Usually, it takes about 12 seconds to process one image with resolution 640×480 into a 3D relief model excluding the import and export time. Figure 3.8 shows the original image, the altered image, the output 3D relief model and a different view angle of the model. In Figure 3.8(d), the arrows denote *x, y, z* coordinates. These examples take the images of the Sphinx (JustEasy 2009) as inputs.

| (a) Input image. | (b) Output image. |

| (c) Output mesh. | (d) Differernt view angle. |
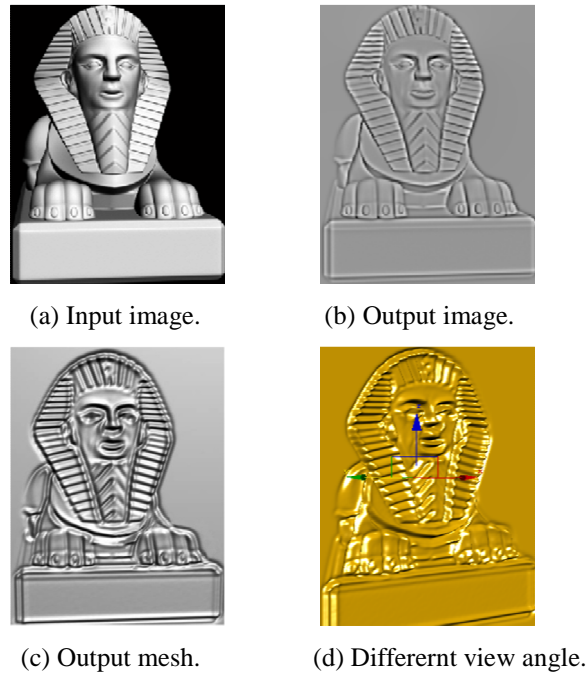
Figure 3. 8 Input image of the Sphinx and results.

Figure 3.9(a) is the input image. Figure 3.9(b), (c) and (d) compare the results generated by the proposed method with ArtCAM and Photoshop to

demonstrate that the proposed algorithm is beneficial for the preservation of edges and enhancement of fine features. It can be seen from Figure 3.9(c) that the neck area is blurred in ArtCAM, whereas in Figure 3.9(b), the ordinary features are preserved with the proposed gradient operation method. ArtCAM produces an image similar to the input where the shape smoothly transits without much flattening. Such smooth transition requires some deep carving in the final relief contradicting the fact that a bas relief is a piece of work carved into a surface with limited depth. The proposed method actually compresses the model into a shallow depth. Figure 3.9(d) shows the bas relief generated by Photoshop transformed to mesh representation. It can be observed that distortion has occurred in the head area, and the facial details have been filtered out.
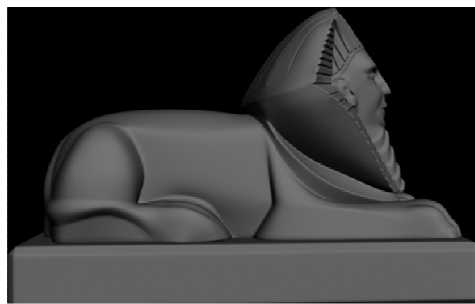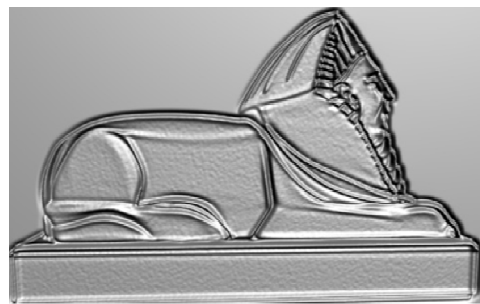
(a) Input image.   (b) Proposed method.
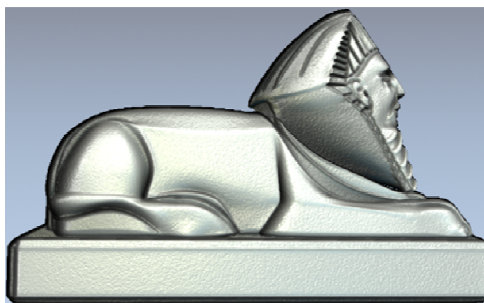
(c) ArtCAM.   (d) Photoshop.

Figure 3. 9 Lateral Sphinx models generated by the proposed methods, ArtCAM and Photoshop.

(a) Wood texture.   (b) Gold texture.

Figure 3. 10 Examples rendered with different textures.
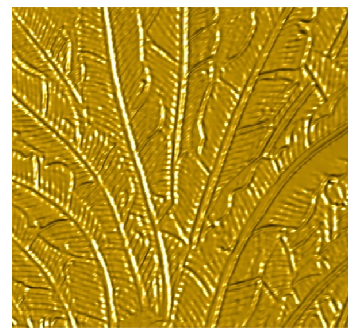
(a1) Input image.   (a2) Output bas relief.
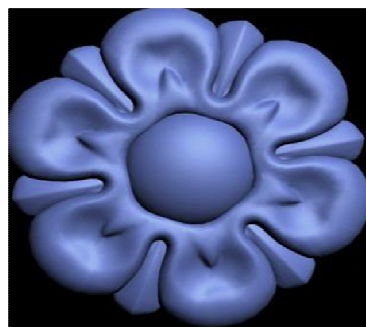
(b1) Input image.   (b2) Output bas relief.
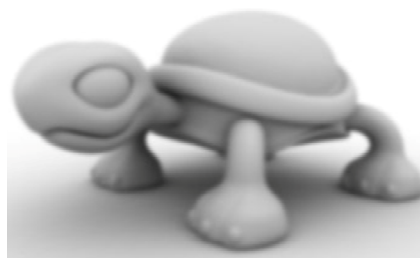
(c1) Input image.   (c2) Output bas relief.

Figure 3. 11 Other examples.

Figure 3.10 shows several rendered images of the proposed method which include different texture effects. The images are rendered with Autodesk|Maya. Figure 3.11 illustrates some other examples. Figure 3.11(a1), (b1) and (c1) are the original input images; Figure 3.11(a2), (b2) and (c2) are the corresponding bas reliefs. The latter demonstrate that the proposed gradient operation method is able to handle both simple plain images (Figure 3.11(b), (c)), and complex colour images (Figure 3.11(a)). The main features being preserved in the results.

3.5 Summary

In this chapter, a series of gradient operations on images have been introduced. These operations sharpen and preserve the features in the final relief model. Compared with existing image processing software, e.g. Photoshop, the proposed approach is able to provide true 3D information rather than a pseudo relief effect which contains "fake" depth information. Noticeable flaws can appear on relief models produced by such image processing software, whereas the proposed method can effectively solve the problem.

The proposed method is able to automatically generate relief models compared to existing techniques such as Shape from Shading(Zeng et al. 2005; Wu et al. 2008), and the generated results can be applied into real application.

CHAPTER 4

RELIEF GENERATION BASED ON 3D MODELS

4.1 Overview

In Chapter 3, bas reliefs have been generated from 2D images by the proposed gradient operation methods. However, the applications of the generated bas reliefs are still confined to some extent. Recently, researchers have developed algorithms which are able to apply image processing techniques to process the height field data from a 3D mesh and finally transform it into a relief. Similarly, the gradient operation based method proposed in Chapter 3 can also be adapted to process the height field data and finally generate bas reliefs. An Alternative approach is provided in this chapter, which attempts to create reliefs (both bas relief and high relief) from 3D meshes directly. The key task is to scale 3D meshes to a certain degree and generate bas reliefs or high reliefs whilst preserving the details in order to produce features that visually appropriate to

reliefs. In this proposed method, firstly, 3D Unsharp Masking (USM) is adopted to enhance the visual features in a 3D mesh, and then a non-linear scaling scheme is developed to generate the final bas relief and high relief.

4.2 Background

Previous relief generation research was mainly concerned with bas relief generation. Those works start with a height field data, and then apply image processing techniques to process the height field data and finally transform it into a relief. This particular work attempts to generate both bas relief and high relief from 3D mesh directly. For high relief generation, scale ratio is over 0.5 according to the definition. It is able to generate high reliefs by a direct linear scaling. Direct linear scaling is easy to achieve, it is also one of the reasons that fewer research works pay attention on high relief generation. This work proposes a method to handle both high relief and bas relief generation. The remarkable contribution is to scale 3D meshes to a certain degree and generate high reliefs while preserving the details. Furthermore, it is beneficial to extend it to bas relief generation as well. A boosting algorithm using Laplacian smoothing operation is adopted to enhance the details. It is essential to understand mesh representing, loading and displaying since the proposed method begins with a 3D mesh, which is outlined as follows.

Meshes store different types of elements including vertices, edges, faces, polygons and surfaces. They can be represented in a variety of ways using different data structure to store the vertex, edge and face data. These include: Face-Vertex Meshes, Winged-Edge Meshes, Half-Edge Meshes, Quad-Edge Meshes, Corner-Table Meshes, and Vertex-Vertex Meshes etc. These methods have particular advantages and disadvantages which were stated by Smith (2006). Face-Vertex mesh represents an object as a set of faces and a set of vertices, which is widely used for mesh representation. Meshes can be stored in

a number of file formats, such as 3DS, DXF, OBJ, PLY, OFF, VRML etc. (Tobler and Maierhofer 2006).

This development is based on a Matlab toolbox provided by Gabriel (2009). A mesh is stored as two matrixes: vertexes store the 3D vertex positions and faces store 3-tuples giving the number of the vertices forming faces.

4.3 Overview of method

The proposed method is depicted in Figure 4.1. When a 3D mesh is provided, in order to flatten its shape without changing its topology whilst preserving its details, the algorithm first applies mesh enhancement by 3D USM (Ritschel et al. 2008; Ihrkea et al. 2009).
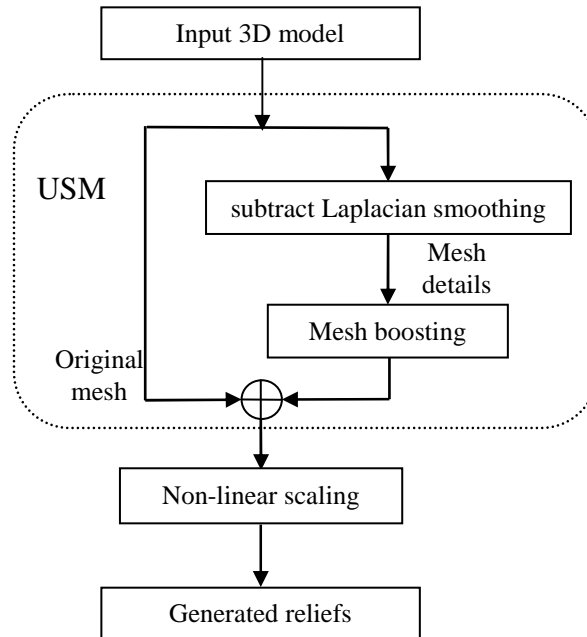
Figure 4. 1 Flowchart of the method.

To implement 3D USM, Laplacian smoothing is subtracted from the original mesh to extract the details of a mesh. The mesh details can be scaled by a

specified factor and added back to the original one to boost the detailed mesh. After boosting the details, a proportional non-linear scaling scheme is developed to achieve final reliefs (bas reliefs and high reliefs).

4.3.1 Mesh enhancement by 3D USM

3D USM is an extension and derivative of 2D Unsharp Masking (Haralick and Shapiro 1992; Hansen et al. 2005; Cignoni et al. 2005; Keith 2009). Its main function is to enhance the contrast of the original mesh. In generic Unsharp Masking, an input signal is enhanced by subtracting the created smoothed version from the original to obtain the high frequency part, which is then linearly scaled by a specified factor and added back to the original one (Luft et al. 2006).

In 3D case:

$$M_{sharp} = M_o + \delta * (M_o - M_{smooth}) \qquad (4.1)$$

M_{sharp} is the sharpened mesh, M_o is the base mesh, M_{smooth} stands for Laplacian smoothing, δ is the amount of enhancement, representing how much the mesh is smoothed which will affect the final relief effects. The adjustment of δ could be useful for artistic controlling.

Laplacian smoothing is adopted to smooth a mesh because this technique changes the position of nodes without modifying the topology of the mesh and also it is attractive for its simplicity (Field 1988; Vollmer et al. 1999). The following section describes Laplacian smoothing in detail.

4.3.2 Laplacian smoothing

Laplacian smoothing changes the position of nodes without modifying the topology of the mesh. More importantly, the Laplacian smoothing is simple to operate since a given vertex only requires information about its immediate neighbours. For each vertex in a mesh, a new position is chosen based on local information and the vertex is incrementally moved there. There are a number of different approximations for the Laplacian operator; each one has its special usage. Desbrun(1999) describes its discrete approximation in Equation 4.2.

$$L(x_i) = \frac{1}{\Sigma w_{ij}} \sum_{j \in N_1(i)} w_{ij}(x_j - x_i) \qquad (4.2)$$

where w_{ij} is the weight for edge defined by (x_i, x_j). There are several schemes to define the weights w_{ij}. They are uniform weight (umbrella operator or combinatorial weight), scale-dependent umbrella operator (distance weight) (Mathieu et al. 1999), tangent weight (Floater 2003) and cotangent weight (harmonic weight). (Sorkine et al. 2004; Alexa 2005; Zhou et al. 2005). Among those schemes, harmonic (cotangent weight) in Equation 4.3 is widely used. According to Desbrun et al. (1999), harmonic weight provides the best smoothing results with respect to shape preservation, minimizing possible distortion related to angle changes.

$$w(i, j) = \cot(\alpha_{i,j}) + \cot(\beta_{i,j}) \qquad (4.3)$$

where $\alpha_{i,j}$ and $\beta_{i,j}$ are the angles opposite to edge (x_i, x_j). Figure 4.2 shows the vertex i and its one-ring neighbours.
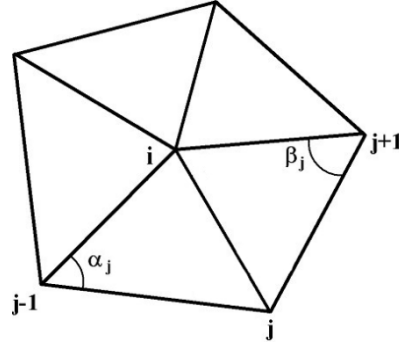
Figure 4. 2 Vertex *i* and its one-ring neighbours.

Laplacian smoothing can be iteratively processed to get the desirable smoothness of a mesh.

4.3.3 Non-linear scaling scheme

To scale 3D meshes efficiently, a non-linear scaling scheme should be proposed instead of linear scaling because simple linear scaling cannot highlight the important part of 3D mesh. In brief, this idea is to scale the height section of the relief proportional to height field. For example, to generate a relief, the higher part of the object should be scaled more, whereas the lower part should be scaled less to preserve the detail. Therefore, the attenuation function (Fattal et al. 2004) can be used to achieve this objective, which is described in Equation 4.4. Scaling Factor(SF) controls the depth compress ratio, where a large value means less compression in depth. For bas-relief generation, a small value is chosen to present the model in a nearly flat plane and a relatively large value applies for high relief. The SF may also related to the preservation of details where a small value of SF would smooth out small depth changes in the model.

$$G(h) = SF * \left(\text{sgn}(h) \frac{a}{|h|} \left(\frac{|h|}{a} \right)^{\beta} \right) \qquad (4.4)$$

The first parameter α determines to what degree height slightly changed. Larger height is scaled more (assuming $0 < \beta < 1$), while smaller height is slightly scaled. Choosing $\alpha = 0.1$ and $\beta = 0.9$ works for the purpose of the scaling as suggested by Fattal et al. (2004).

4.4 Relief generation

4.4.1 High relief generation

In high reliefs (alto relievo), the forms have over half of their natural depth attaching to a surface or separating from it.
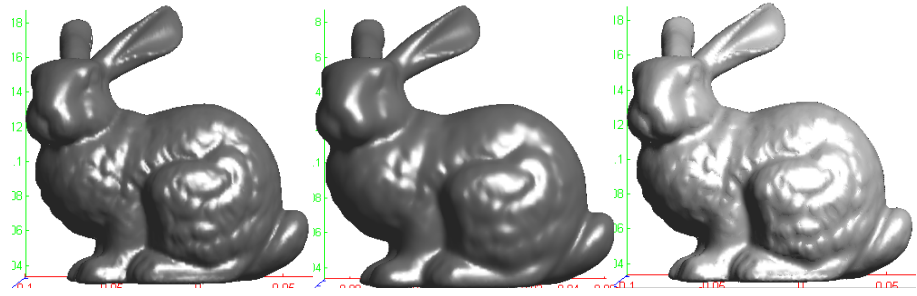
(a) Input bunny model.   (b) Smoothed bunny model.   (c) Sharpened bunny model.

(d)SF=0.7.   (e) SF=0.6.   (f) SF=0.5.
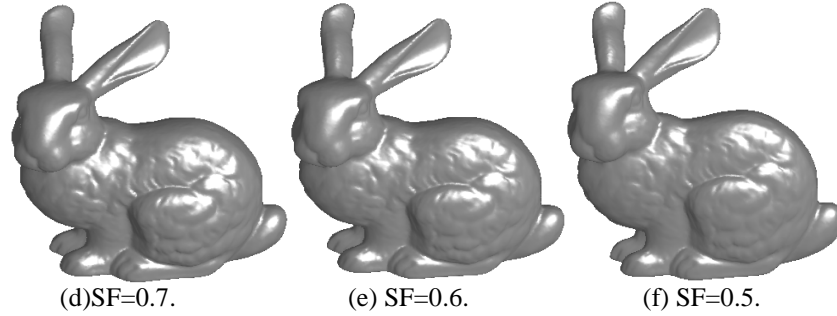
Figure 4. 3 High reliefs with Bunny model. (a), (b), (c) represent the input Bunny model, smoothed model and unsharp model respectively. (d), (e), (f) are different final relief result with parameters.

Therefore, Scaling Factor (SF) is defined as over 0.5 according to the definition.

Bunny and Skull are taken as examples to illustrate the results of the algorithm. For high relief generation, the parameters are set as follows: δ=0.2, SF=0.7, SF=0.6, SF=0.5. All the models are from Aim Shape (2009).

Figure 4.3 and Figure 4.4 present the results of high reliefs. It can be seen that higher SF (SF=0.7) preserve more features.

(a) Input skull model.   (b) Smoothed skull model.   (c) Sharpened skull model.

(d) Rendering and lighting skull model.

Figure 4. 4 High reliefs with Skull model. (a), (b), (c) represent the input Skull model, smoothed model and unsharp model respectively. (d) the final rendered skull relief with frame.

However, the overall details are preserved for all SF. The influence of δ will be examined in Section 4.4.4.

4.4.2 Bas relief generation

It is noted that the proposed algorithm works for high relief in Section 4.4.1. In bas reliefs, the forms have under half of their natural depth always attaching to a surface. Recent researchers take 0.02 as compression ratio. Figure 4.5 demonstrates the bas reliefs of bunny model and skull model generated by the proposed method with the parameters: δ=0.2, SF=0.02. It can be observed that the proposed mesh enhanced techniques and non-linear scaling scheme can effectively preserve the details of the generated bas relief results.
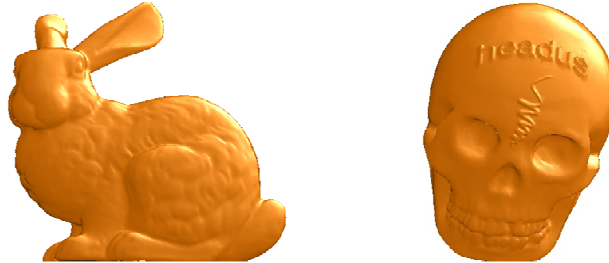
Figure 4. 5 Bas reliefs generated by the proposed algorithm: Bunny and Skull.

Figure 4. 6 The bas relief generated by the proposed algorithm: Vase lion and rendered Vase lion with frame.

Figure 4.6 gives another example to show performance of the proposed algorithm. It can be seen that it is able to generate bas relief with details preserved.

4.4.3 Different view angles

(a1) Initial lion model.

(b1) bas relief with frame.

(a2) Front-view lion model.

(b2) Front-view bas relief with frame.

(a3) Left-view lion model.

(b3)Left-view bas relief with frame.

(a4) Back-view lion model.

(b4) Back-view bas relief with frame.

Figure 4. 7 Reliefs of Different view angles of Chinese lion.

It is easier to apply different view angles from different view directions for the original model because the proposed method operates on 3D meshes directly. For example (see Figure 4.7), adjusting the position of the model and then

applying the proposed algorithm can easily get different view angles of relief generation.

4.4.4 Parameter testing

The main factor influences the results and determines the appropriate parameter is tested in this section. Bas relief generation with Skull model is taken as an example. In the proposed method, δ is the amount of enhancement, represents how much the mesh is smoothed which will affect the final relief effects.

SF=0.02 δ=0.2

SF=0.02 δ=0.5

SF=0.02 δ=1.0
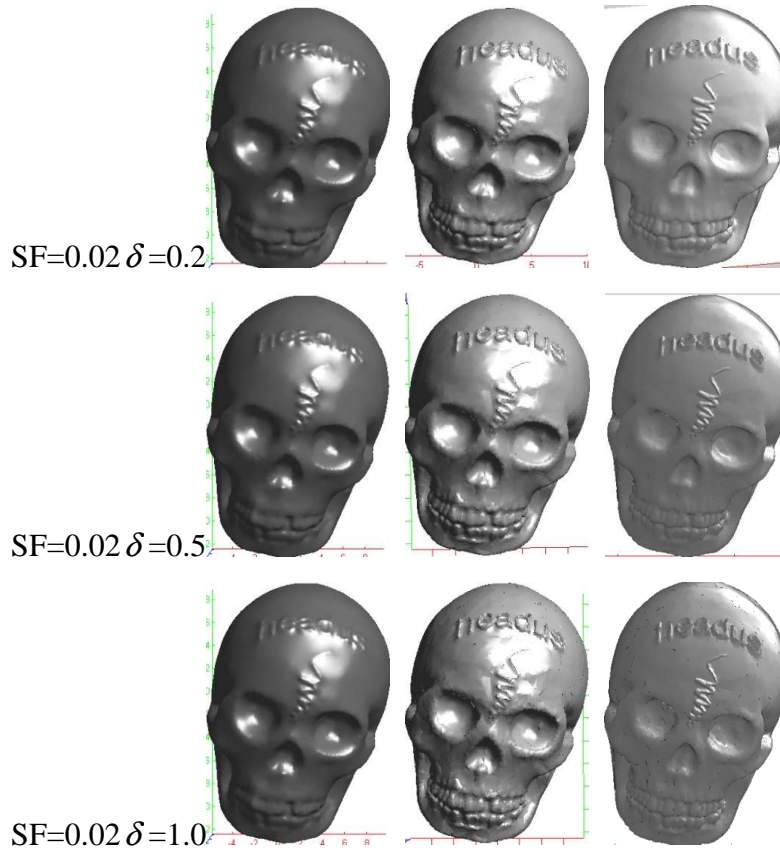
Figure 4. 8 Different δ from 0.2 to 1.0.

It can be seen from Figure 4.8 that with the increasement of δ, the relief result is enhanced. However, the larger δ results in undesired deformation when applied to 3D USM. In a generic Unsharp Masking, the high frequency part is

53

linearly scaled by a specified factor and added back to the original one. A suitable specified factor, in this case δ should be chosen carefully because artifacts are triggered by a larger δ in the final bas relief generation as Figure 4.7 indicates. It is noted that δ =0.2 can produce the pleasing results.

4.5 Summary

In this chapter, the algorithm which can produce reliefs directly on 3D meshes has been implemented and tested. 3D Unsharp Masking and the non-linear scaling scheme have been developed to generate bas relief and high relief. The results have shown that the proposed methods can preserve the details of the generated bas reliefs and high reliefs. Compared with existing works(Kerber et al. 2009; Sun et al. 2009; Weyrich et al. (2007)), the proposed method is relatively easy to implement since it operates 3D meshes directly.

CHAPTER 5

DIGITAL SUNKEN RELIEF GENERATION BASED ON 3D MODELS

5.1 Introduction

Sunken relief is the third type of relief sculpture, also known as intaglio or hollow relief; the objects are carved into a flat surface. Sunken reliefs often utilise the engraved lines or strokes to strengthen the impression of a 3D presence and to highlight the features which otherwise are unrevealed. Compared with other (high reliefs and bas reliefs) relief forms, sunken reliefs highlight the depth perception more strongly. Despite an increasing amount of research on digital relief generation in computer graphics, little attention has been paid on the generation of the abstract sculpture form using pure engraved lines. Two types of sunken relief generation have been developed in this chapter; one is created with pure engraved lines, which is outlined in Section

5.4, the other attempts to create sunken reliefs incorporating the contour lines seamlessly with the smooth surfaces, which is outlined in Section 5.5.

5.2 Background

Among three types of relief, sunken reliefs lie largely on the shape which do not protrude from the surface, but are carved into the surface. In ancient Egypt, sunken relief was commonly used to illustrate stories and show the greatness of the pharaoh (as shown in Figure 5.1). It is noticed that the lines of contours are vivid elements of great importance to present this special stylization. It is also used for inscriptions and engraved gemstones. Nowadays, sunken reliefs can be used to decorate the surfaces of furniture, walls, buildings, and jewellery.

Figure 5. 1 A sunken relief of ancient Egypt (Artist Unknown, 1336 BC).

To produce a sunken relief, the sculptor carves the relief within a deeply incised line. As a result, the contours are sunk below the surrounding surface whilst leaving the highest parts on the surface level. Figure 5.1 shows that the feature lines are important for depicting the edges of the objects, such lines represent most visual features of a sunken relief sculpture. Because lines are flexible and concise, they are considered as the best way to represent general and abstract figures.

56

Lines play an important role in sunken reliefs. Rogers (1974) introduced the definition of external contours and internal lines of sunken relief. External contours are defined as the principal lines, which are determined by the shape of the object itself and the viewer's perception. In addition, several other linear features may be presented in a relief. These are usually referred to as the interior lines because they are all contained within the overall shapes bounded by the external contours. Edges formed due to the connection of planes/surfaces at an angle may be rendered sharply so that they become a linear feature. These internal feature lines are defined as the secondary lines in a real sunken relief. Last but not the least, there are lines which are not derived from the 3D form of the relief, but are overlaid to highlight the primarily graphic features.

Most existing research on relief generation is concerned with creating a smooth relief surface from either image or geometry input. Such a surface has a shallow depth but can deceive human perception to a real 3D shape with a much greater depth ratio. Previous work has paid little attention to the importance of lines (Kerber et al. 2009; Sun et al. 2009.). The proposed methods start from a full scale geometric mesh of a 3D object. Therefore, the user can benefit from abundant 3D models available either online or from laser scanning. This method is the first to implement sunken relief generation by uniquely including feature lines in relief creation, which distinguishes this work from its predecessors (Kerber et al. 2009; Sun et al. 2009; Weyrich et al. (2007)). The sunken relief results seem promising, however in order to model the sunken relief with smooth transition between lines, a combination of three different inputs has been proposed: a line drawing image provides input for contour lines; a rendered Lambertian image shares the same light direction of the relief sets the visual cues; and a depth image conveys the height information. It is able to maximise the presence of features in a sunken relief

by matching the target relief surface with the three given input images by an optimization process

5.3 3D line drawings

5.3.1 Lines in sunken relief and 3D Line drawings

Line drawings refer to extracting lines (the most obvious features of the model) from 3D models. The extracted lines can be applied to artistic stylization and abstraction work with applications ranging from illustrations to cartoons and gaming scenes. This work is inspired by line drawings from 3D models since sunken reliefs depend considerably on the carved lines in conveying the surface shape. Lines also convey other different things, including various combinations of lighting, materials, surface markings, and discontinuities (Rusinkiewicz et al. 2008).

Koenderink (1984) explained the concept of contours and its connection to human perception. Such contours in line drawings are analogous to the principle lines in sunken reliefs. Later on, creases were used, which was regarded as a big improvement for line drawings from 3D objects (Markosian et al. 1997; Raskar 2001; Kalnins et al. 2002). Creases are sharp features defined on the mesh surface. Suggestive contours (Decarlo et al. 2003; Sousa and Prusinkiewicz 2003; Decarlo et al. 2004), which are analogous to the interior lines in sunken reliefs, are minor on-surface features similar to contours that are view dependent and help denoting the local shape. Other drawing elements, such as hatching, are prevalent in more sophisticated line drawings. Many small lines can be combined in such a way that they simultaneously stylise the tone and material (Cole et al. 2008 and 2009). For a more detailed review on line drawings, please refer to Rusinkiewicz et al. (2008).

5.3.2 Line drawings algorithm

Two types of lines are included in line drawings: contours (occluding contours and silhouettes) whose definition is view-dependent and suggestive contours whose definition depends on the higher-order differential properties. Object-space algorithm developed by Decarlo et al. (2003) is adopted to extract line drawings. A brief summary of the algorithm is shown below.

Contours: A smooth surface is provided, the contour lines are defined as a set of points that lie on the surface and whose surface normal is perpendicular to the view vector:

$$\mathbf{n(p)} \cdot \mathbf{v} = 0 \tag{5.1}$$

$\mathbf{p}$ is a point on the surface, $\mathbf{n}$ is its normal and $\mathbf{v}$ is the view vector. This set of points form disconnected curves on the surface. By projecting the visible part of the lines onto the image plane, a line drawing is produced which is defined by the occluding contours and silhouettes.

Suggestive contours: Suggestive contours relate to the ridges and valleys as inflection points from a particular view on the surface, which involve computation of the local extrema of the curvature. A direction vector $\mathbf{w}$ is defined as the projection of view vector on the tangent plane at point $\mathbf{p}$.

$$\mathbf{w} = \frac{\mathbf{v} - (\mathbf{n(p)} \cdot \mathbf{v}) \cdot \mathbf{n(p)}}{\left\| \mathbf{v} - (\mathbf{n(p)} \cdot \mathbf{v}) \cdot \mathbf{n(p)} \right\|} \tag{5.2}$$

It is noted that the local minima of $\mathbf{n(p)} \cdot \mathbf{v}$ in direction $\mathbf{w}$ suggests a possible location on a ridge/valley. This local minima corresponds to the zero value of

the derivative of $\mathbf{n(p)} \cdot \mathbf{v}$ along direction $\mathbf{w}$ at point $\mathbf{p}$ where the second order derivative along direction $\mathbf{w}$ is positive:

$$\nabla_w(\mathbf{n(p)} \cdot \mathbf{v}) = 0 \text{, and}$$

$$\nabla_w \nabla_w(\mathbf{n(p)} \cdot \mathbf{v}) > 0 \tag{5.3}$$

where ∇_w denotes the directional derivative along $\mathbf{w}$. This condition is also equivalent to the zero value of radial curvature κ_r along direction $\mathbf{w}$ where the directional derivative along $\mathbf{w}$ of the radial curvature is positive:

$$\kappa_r = 0 \text{, and}$$

$$\nabla_w \kappa_r > 0 \tag{5.4}$$

The suggested contours are generated by projecting those points on the surface that satisfy the aforementioned condition.

There is a large body of literature addressing the problem of extracting line drawings from exiting 3D models (Kalnins et al. 2002; Decarlo et al. 2003; Cole et al. 2008). Many works contribute to the generation of different stylization and content related line drawings, which is beyond the scope of discussion in this work. As the lines in sunken reliefs highlight the contours, extracting the plain line drawings is the necessity. Stylization is not needed.

This development is mainly based on the existing work developed by Rusinkiewicz et al. (2008) to obtain lines drawings from 3D models. It is noticed that directly applying the output is not suitable for generating relief-style sculptures, since there are some unexpected breaks in the contours and

dots by noise (as shown in Figure 5.2(b)) or too many line details (as shown in Figure 5.4(a)). Additional pre-processing is introduced to tidy up the image.

In general, there are two alternative ways to achieve pre-processing; these depend upon the type of model. For models with smooth surface like the horse in Figure 5.2(a), digital image processing is highly efficient, easy to implement and can produce good results. For models with many local variations, mesh operations like smoothing can be applied (as shown in Figure 5.3).

5.3.3 Pre-processing: Image processing

Image processing can be applied to the extracted line drawings to enhance their quality for further processing. The advantage of applying digital image processing is that it is fast and easy to implement. Figure 5.2(a) shows the input horse model.

Smooth, concise and successive boundary lines are expected in relief artwork. It can be seen from Figure 5.2(b) that there are some breaks and noises which are not appropriate for relief-style sculpture generation.

Removing minor noise is the first necessary step to emphasise lines in the sculpture. An effective and simple way to achieve the desired goal is to apply erosion (as shown in Figure 5.2(c)).

The next step is to recover the image by dilating the image to fix the holes and breaks and to achieve the final image as shown in Figure 5.2(d).

Both erosion and dilation can be repeated several times until required results are achieved.
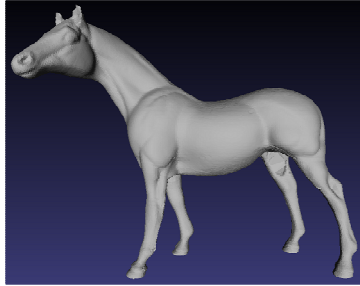
(a) Input horse model.
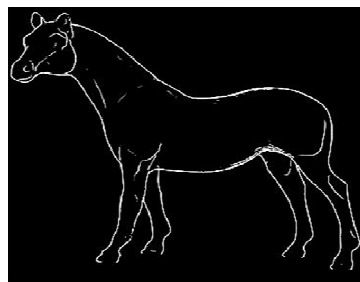
(b) Converted image of line drawings.
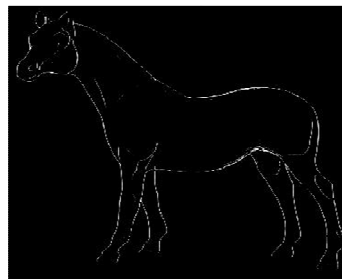
(c) Lines after erosion.
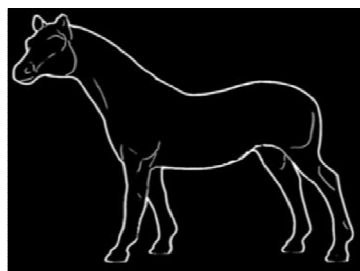
(d) Lines after dilation.

Figure 5. 2 Image processing example of generated lines of the horse model.

5.3.4 Pre-processing: mesh smoothing

For some models like the bunny, there are too many small local variations as shown in Figure 5.3. Therefore, it is necessary to pre-process the mesh and extract the lines afterwards. This is to control the density of the lines and thus to influence their presence in the final relief sculpture. It is better to smooth the mesh to get rid of some details if required and to make the final relief-style sculpture as clear as possible. Taking the bunny model as an input, Figure 5.4(a) shows the extracted lines of the initial model; it is noticeable that there are so many details which require much effort during the final sculpture generation. To overcome this issue, the user is provided with a tool to control the input by filtering out some details if required. Laplacian smoothing operator was chosen to remove those unwanted strokes in the selected area. There are a number of different approximations for the Laplacian operator; each has its special usage. Desbrun (1999) describes its discrete approximation.

$$L(x_i) = \frac{1}{\Sigma w_{ij}} \sum_{j \in N_1(i)} w_{ij}(x_j - x_i)$$

(5.5)

where w_{ij} is the weight for edge defined by (x_i, x_j). There are several schemes to define the weights w_{ij}. As discussed in Section 4.3.2, cotangent weight $w(i, j) = \cot(\alpha_{i,j}) + \cot(\beta_{i,j})$, is used.

An example of the practice of controlling the stroke density is shown in Figure 5.4(b), (c) and (d) after 3 different levels of smoothing. Users can control the iterative number of smoothing to gain the effects they expected by removing some details.

Figure 5. 3 Bunny model.

(a) Lines output without smoothing.   (b) First time smoothing.
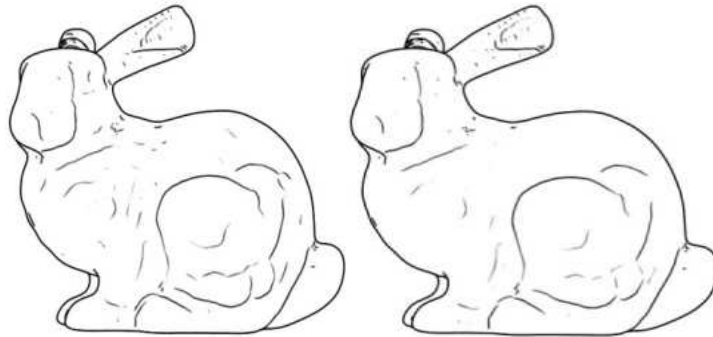
(c) Second time smoothing.   (d) Third time smoothing.

Figure 5. 4 Line drawings of bunny model with different levels of smoothing

5.4 Sunken relief generation using featured lines

Lines are firstly extracted by line drawings from a given 3D object according to Section 5.3, and a pre-processing process is applied to the line drawings to clear the unwanted noise for the relief generation according to different types

of models. For simple models with less local variations, digital image processing can be applied supplely. Alternatively, for models with fine local details, a Laplacian smoothing step can be applied to the geometric model to remove some unwanted details before the line drawings extraction.

After obtaining the required line information, the mesh of a 3D relief-style sculpture can be generated. The x and y components of each vertex position correspond to the location of their counterpart in the line image I. The z components are derived from the entries; this operation is explained as follows:

$$z = SF * (I(x, y) - os) \tag{5.6}$$

where $I(x, y)$ is the image pixel value after the aforementioned pre-processing, which corresponds to depth z, os is the offset value and SF is the Scaling Factor. This leads to a sculpture in which the background is mapped to a zero-level and each line is carved deeper into the material, the depth is controlled by the Scaling Factor.

Pre-processing can be treated as a specially designed filter which controls the quality and stylization of the final sculpture effects. To give an example, Figure 5.5(a) and 5.5(b) are created with images of Figure 5.4(a) (without smoothing) and 5.4(d) (with smoothing) respectively: although the same initial 3D geometry of the bunny is used, both sculptures exhibit different stylization with varying line densities.

It can be seen from Figure 5.5(b) that the generated bunny sunken relief model bears the main shape features with sufficient details not to distract the viewer with too many small strokes.

(a) Result without smoothing.

(b) Result with smoothing

Figure 5.5 Comparison of reliefs with different line density.

Figure 5.6 demonstrates that the proposed technique works for both simple and complex objects. For example, it can be seen from the golf ball model that the variation of lines can convey a convincing 3D geometric variation of depth even though they are engraved into a flat surface.
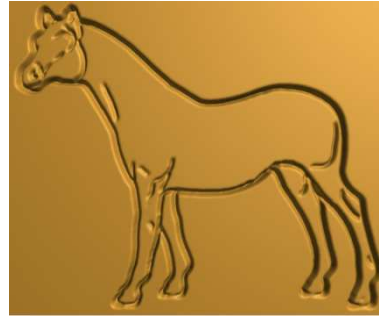
(a) Horse model.
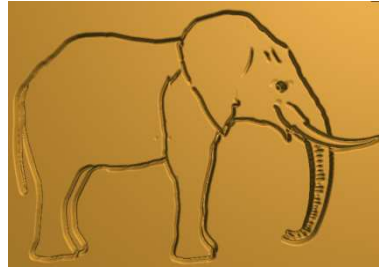
(b) Elephant model.
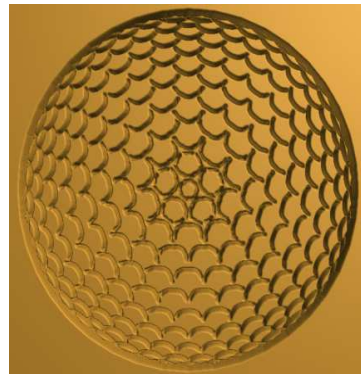
(c) Golf model.

Figure 5. 6 Reliefs generated with the proposed method.

5.5 Advanced sunken relief generation using multiple inputs

3D line drawings algorithm can be used to extract exactly the lines needed in generating the edges of a sunken relief as introduced in Section 5.3.2. However, transforming them into a 3D carving in conjunction with smooth height transition is an unsolved problem. Sunken reliefs generated in Section 5.4 are promising; however, to generate a realistic sunken relief, the smooth height transition between edges is also essential. Both the lines and the height transition have to be combined together to emphasize the presence of a 3D object. The method presented in this section is different from that in Section 5.4. It combines the line drawings input with height generation that visually highlights the shape features on the generated sunken reliefs.

5.5.1 Three inputs

A 3D surface carries more information than a single image does. The implementation starts from a triangular mesh by translating it into multiple inputs: a picture of plain line drawings (as illustrated in Section 5.3), an image rendered using Lambertian shading, and a depth image. These inputs are combined together in a composition procedure to produce the final relief art piece. These procedures are illustrated in Figure 5.7. The input of line drawing helps to create feature lines in the sunken reliefs at the desired places. The other two inputs work in a complementary manner to maintain a smooth relief surface.
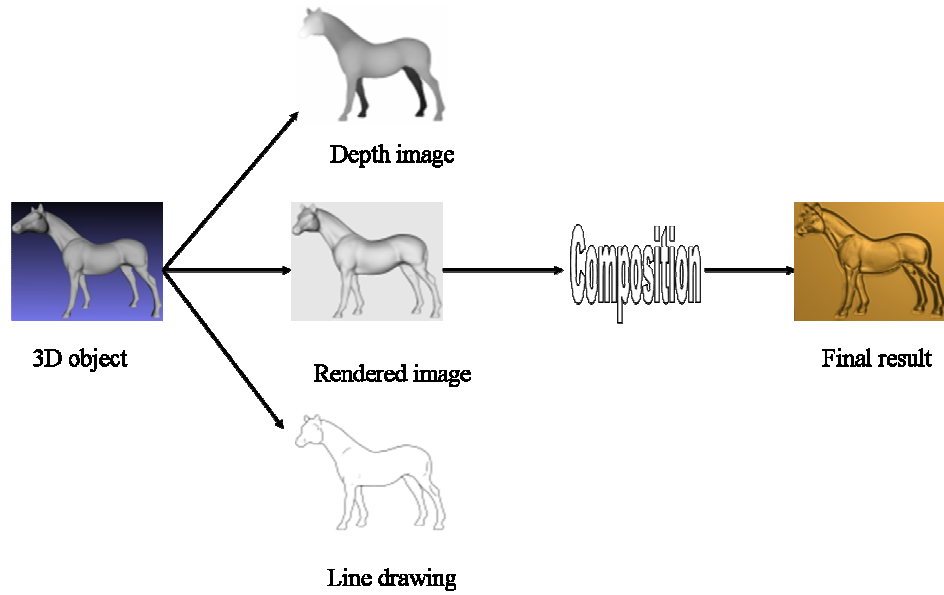
Figure 5. 7 Procedures of the proposed method.

Depth Image Input

It is beneficial to start from a 3D mesh as it provides the height information. Belhumeur et al. (1999) suggested that a linear compression of the height could lead to ambiguity for some particular view points of the generated relief. Instead of using the simple linear compression approach, optimization approaches have been developed in Section 5.5.2 to ensure a robust solution. Using the height information as input, the depth is simply rendered on the image projection plan as a grey image.

Lambertian Shading Input

Images rendered with the Lambertian model are used as one input source to help recover the height information in the relief. The pixel value I is computed from the dot product of normal **n** and light direction **m** which point from the surface point toward the light source:

$$I = \alpha(\mathbf{n}(\mathbf{p}) \cdot \mathbf{m}(\mathbf{p}))$$

<div align="right">(5.7)</div>

where α is the intensity of the light.

Image I implicitly codes the surface normal at each point; it helps to recover the height information as the change of the normal provides essential information for the perception of the human eyes. In practice, the light source is aligned with the view point, which means $\mathbf{n}(\mathbf{p}) \cdot \mathbf{v}$ is actually rendered. In the production process, the light direction can be aligned with the real setting for the relief display accordingly to allow the albedo of the generated relief in line with the geometry exactly.

Line drawings Input

The input of line drawing helps create feature lines in the sunken reliefs at the desired places. Line drawing algorithm has been explained in Section 5.3. It is noticed that the direct use of line drawings cannot guarantee good results, so a necessary pre-processing should be done beforehand. After obtaining a picture of plain line drawings, it can work together with the other two inputs to create the advanced sunken relief effects.

5.5.2 Relief Height Generation

To generate a relief, the inputs are initiated by translating a 3D object into three separate images: a line drawing, a Lambertian shaded image, and a depth image. Those images are generated from the same view point and on the same projection plane to ensure that they are perfectly aligned with each other in terms of their x, y coordinates in the pixel domain. The image is set to have a size of m by n.
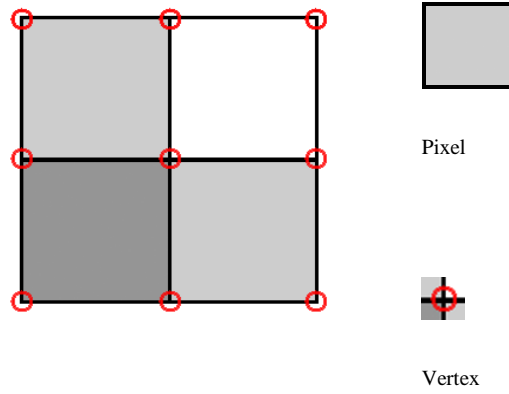
Figure 5. 8 The surface discretization of the relief in relation to pixels of an input image, where red circles represent the vertices' locations right on the corners of pixels.

In a classic fashion, the discrete surface of a relief is created from an array of points that are aligned with the pixels in the input image and their height is adjustable accordingly to generate a smoothly shaded surface. Alexa and Matusik (2010) suggested a new arrangement of using four connected triangles to calculate the value at a given pixel, where a pixel of the input image is modelled as a small pyramid in the relief. A staggered layout is selected as shown in Figure 5.8, where the actual relief grid for storing height data is selected by shifting the pixel grid in x and y directions for half a pixel size.

The pixel value of the relief grid node (the red circle in Figure 5.8) at (x, y) is defined by averaging the values of its four pixel neighbours,

$$I(x, y) = \frac{1}{4}\left(I(x - \frac{1}{2}, y - \frac{1}{2}) + I(x - \frac{1}{2}, y + \frac{1}{2}) + I(x + \frac{1}{2}, y - \frac{1}{2}) + I(x + \frac{1}{2}, y + \frac{1}{2}) \right)$$

(5.8)

The gradient operation of the intensity at the given grid location (x, y) is defined using the same four pixel values as

71

$$\nabla I = \begin{pmatrix} \dfrac{\partial I(x,y)}{\partial x} \\ \dfrac{\partial I(x,y)}{\partial y} \end{pmatrix}$$

$$= \begin{pmatrix} \dfrac{1}{2}\left(I(x+\tfrac{1}{2},y-\tfrac{1}{2}) + I(x+\tfrac{1}{2},y+\tfrac{1}{2}) - I(x-\tfrac{1}{2},y-\tfrac{1}{2}) - I(x-\tfrac{1}{2},y+\tfrac{1}{2}) \right) \\ \dfrac{1}{2}\left(I(x+\tfrac{1}{2},y+\tfrac{1}{2}) + I(x-\tfrac{1}{2},y+\tfrac{1}{2}) - I(x+\tfrac{1}{2},y-\tfrac{1}{2}) - I(x-\tfrac{1}{2},y-\tfrac{1}{2}) \right) \end{pmatrix}$$

(5.9)

Alternatively, the gradient operation of the height value can be defined at the pixel location in a similar compact fashion when the surface normal is estimated by Lambertian Image. Such compact layout helps to increase the resolution for the reconstruction of the relief surface. The following section describes the method to derive an independent energy function for each of the aforementioned inputs.

Depth Input

With respect to the input depth image, it is able to transform it into a piece of relief by a linear compression. Such direct operation may cause loss of the local features and the resulting relief look dull due to lack of depth information incorporated. The height information is processed with a non-linear compression by recovering the surface from computing the Poisson equations. The depth value is denoted at position (x, y) as $I_d(x, y)$. The second order derivative value is computed by:

$$g = \nabla \cdot G(\nabla I_d)$$

(5.10)

G is a non-linear high dynamic compression function, which takes the following form:

$$G(a) = \left(\text{sgn}(a) \frac{\gamma}{|a|} \left(\frac{|a|}{\gamma} \right)^{\beta} \right)$$

(5.11)

γ and β jointly control the compression ratio. $\gamma=0.1$ and $\beta=0.9$ are set in this experiments.

Then the relief surface is reconstructed by solving the following Poisson equations,

$$\nabla^2 h(x, y) - g = 0 \tag{5.12}$$

$h(x, y)$ specifies the discrete height. This Poisson equation can be numerically resolved. However, in order to integrate this solution with all three inputs, the energy terms is defined and the solution is found by minimizing the overall energy.

Therefore, the energy term is formed that relates to the depth image input as follows:

$$E_d = \sum_{x=2}^{m-1}\sum_{y=2}^{n-1}\left(\begin{array}{l}h(x+1, y) + h(x-1, y) + h(x, y+1)\\ + h(x, y-1) - 4h(x, y) - g(x, y)\end{array}\right)^2 \tag{5.13}$$

Lambertian Image Input

$\mathbf{L}$ is denoted as the light source. $\mathbf{L}=\alpha\mathbf{m}(\mathbf{p})$, where α is the light intensity and $\mathbf{m}$ is the light direction at point $\mathbf{p}$. The albedo (or the reflection radiance) at the point is

$$I = \mathbf{L}\cdot\mathbf{n} \tag{5.14}$$

with n as the surface normal at the point.

Using the staggered grid layout as shown in Figure 5.8 estimates the reflection radiance I of the relief at a pixel point $(x+1/2, y+1/2)$, the four height values at

the pixel's corners can be used to compute the normal direction first. The estimated normal can be written as

$$\mathbf{n} = \begin{pmatrix} n_x \\ n_y \\ n_z \end{pmatrix} = \frac{1}{\hat{n}} \begin{pmatrix} -\dfrac{\partial h}{\partial x} \\ -\dfrac{\partial h}{\partial y} \\ 1 \end{pmatrix}$$

(5.15)

where

$$\frac{\partial h}{\partial x} = \frac{1}{2}\left(h(x+1,y)+h(x+1,y+1)-h(x,y)-h(x,y+1)\right), \quad \frac{\partial h}{\partial y} = \frac{1}{2}\left(h(x,y+1)+h(x+1,y+1)-h(x,y)-h(x+1,y)\right)$$ and

$$\hat{n} = \sqrt{1 + \left(\frac{\partial h}{\partial x}\right)^2 + \left(\frac{\partial h}{\partial y}\right)^2}$$ as the scale factor to normalise the normal vector. In the latter optimization steps, linearising the system is necessary by estimating the scale factor with the results from the previous iteration rather than computing it at the current time. The scale factor is initiated as 1 when computing starts. $\mathbf{n}$ is given as the normal to compute the reflection radiance pixel by pixel using Equation 5.14.

The input Lambertian image has the intensity value at a given position ($x+1/2$, $y+1/2$) as $I_L(x+1/2, y+1/2)$. Recalling the staggered grid setting, it is noted that both the estimated reflection radiance and the intensity image are defined at the pixel grids and their gradients are defined at the relief grid nodes by Equation 5.9. Using the image gradient compression method introduced by Fattal et al. (2002), I can get the compressed image gradient of the input as $G(\nabla I_L)$, where the compression function is defined in Equation 5.11. The gradient of the reflection radiance is expected identical to the compressed input value, that is

$$\nabla I(x, y) - G(\nabla I_L) = 0$$

(5.16)

74

Therefore, it is defined the related energy term to the Lambertian image input as follows,

$$E_L = \sum_{x=1}^{m-1}\sum_{y=1}^{n-1}\left(\frac{1}{2}\left(I(x+\frac{1}{2},y-\frac{1}{2})+I(x+\frac{1}{2},y+\frac{1}{2})-I(x-\frac{1}{2},y-\frac{1}{2})-I(x-\frac{1}{2},y+\frac{1}{2})\right)-G(\frac{\partial I_L}{\partial x})\right)^2$$
$$+\sum_{x=1}^{m-1}\sum_{y=1}^{n-1}\left(\frac{1}{2}\left(I(x+\frac{1}{2},y+\frac{1}{2})+I(x-\frac{1}{2},y+\frac{1}{2})-I(x+\frac{1}{2},y-\frac{1}{2})-I(x-\frac{1}{2},y-\frac{1}{2})\right)-G(\frac{\partial I_L}{\partial y})\right)^2$$

(5.17)

Line Drawing Input

A separate line drawing input layer is included in order to generate the engraved line effect for a sunken relief. Another energy item specially associated to this input is defined. The line drawings are provided, firstly, initiate a stencil based on it. The stencil is an image whose strokes are one pixel wider than those in the input. *Iw* (*x*+1/2, *y*+1/2) is denoted as the pixel value at position (*x*+1/2, *y*+1/2) of the line drawings input. The relief grid value *S(x, y)* of the stencil template is defined as follows,

$$S(x,y)=\begin{cases} 1 & if \quad \sum_{i=x-\frac{1}{2}}^{x+\frac{1}{2}}\sum_{j=y-\frac{1}{2}}^{y+\frac{1}{2}} I_w(i,j) > 0; \\ 0 & else \end{cases}$$

(5.18)

The stencil value is zero only when all of its four neighbouring pixels are zero.

Using stencil *S* can filter out the influence of those pixels which are not adjacent to a given stroke to avoid unnecessary computation. In order to engrave lines on the relief according to the line drawings input, it is expected that the following relationship holds.

$$S \cdot \left(\nabla I(x,y) - G(\nabla I_w)\right) = 0$$

(5.19)

I being the intensity of the reflection radiance calculated by Equation 5.14 whose values are defined at the pixel grid and whose gradients are defined at the relief grid and *G* is the non-linear compress function of Equation 5.11.

Therefore, the definition of the energy term for the line drawings input is described as,

$$E_w = \sum_{x=1}^{m-1}\sum_{y=1}^{n-1} S(x,y)\left(\frac{1}{2}\left(I(x+\frac{1}{2},y-\frac{1}{2})+I(x+\frac{1}{2},y+\frac{1}{2})-I(x-\frac{1}{2},y-\frac{1}{2})-I(x-\frac{1}{2},y+\frac{1}{2})\right)-G(\frac{\partial I_w}{\partial x})\right)^2$$
$$+ \sum_{x=1}^{m-1}\sum_{y=1}^{n-1} S(x,y)\left(\frac{1}{2}\left(I(x+\frac{1}{2},y+\frac{1}{2})+I(x-\frac{1}{2},y+\frac{1}{2})-I(x+\frac{1}{2},y-\frac{1}{2})-I(x-\frac{1}{2},y-\frac{1}{2})\right)-G(\frac{\partial I_w}{\partial y})\right)^2$$

(5.20)

Compositing Relief by Minimizing the Energy

To recover the height information, the superposition of all existing energy terms with respect to the height values at the corners of the pixels has to be minimized. The overall energy is written as follows:

$$E = w_d E_d + w_L E_L + w_w E_w$$

(5.21)

This illustrates that the weighting coefficients control the influence of each term. The gradient of the reflection radiance non-linearly depends on the height alternation. This dependency is linearised by estimating the scale factor which normalises the normal vector by the results from the previous optimization step.

The optimization problem is defined as,

$$\min_{h<0,\ -h<h} E$$

(5.22)

The constraints of height ensure the relief is sunk into a given flat plane. h_{max} explicitly specifies the maximum depth that can be carved into the plane.

An alternative way of regulating the relief carving depth is to penalise the small height value. It can be achieved by including an additional energy item Eh into the overall energy computation.

$$E_h = \sum_{x=1}^{m} \sum_{y=1}^{n} \left(h(x, y) - h^* \right)^2$$

(5.23)

with $h^* = -\theta \log(1 - \theta h(x, y))$, where θ controls the degree of compression.

5.5.3 Results

The proposed algorithm is capable of providing relief models as triangular meshes. Such meshes can be further simplified for less storage or to lower the computational cost for future operation. Other post-processing steps, such as texturing and shading can be added to create further embellished results.

As shown in Figure 5.9(a), a plain carved relief generated only includes the line drawings input. Figure 5.9(b) and (c) represent the composting results with all inputs. They have different depths of carving. It can be observed that combining both lines and the surface together can produce more advanced sunken reliefs.

(a) Lines only.

(b) Shallow depth.

(c) Deep depth.

Figure 5. 9 Comparison of reliefs with different inputs.

Figure 5.10 compares the results from different line drawings inputs with and without Laplacian smoothing. It can be seen that redundant strokes of input cause the result (Figure 5.10(a)) appear bumpy and hide the main shape features at some point, which can be improved (see Figure 5.10(b)) with a

mesh smoothing process before extracting the contour lines when preparing the line drawings input.

(a) Initial lines input.   (b) Laplacian smooth.
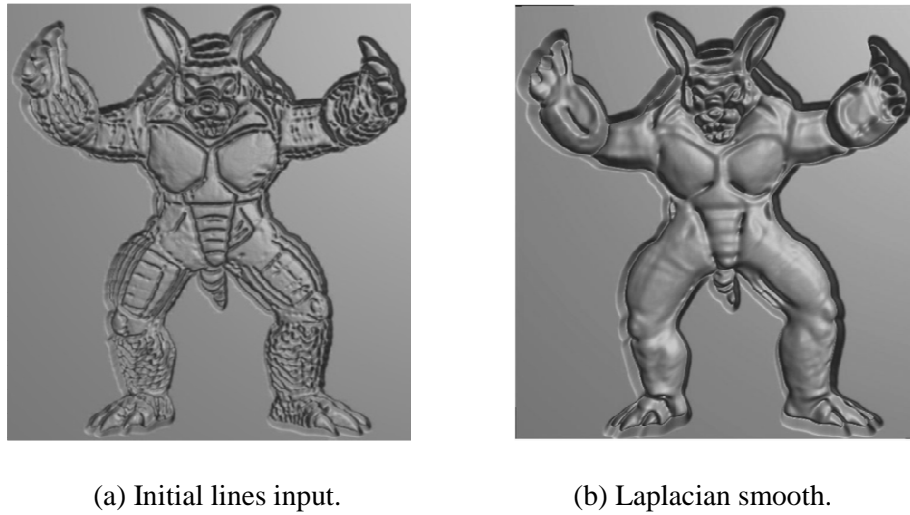
Figure 5. 10 Comparison of reliefs with different line density.

Figure 5.11 demonstrates the generated bas reliefs (a) by Cignoni et al. (1997), (b) Kerber et al. (2007), (c) Kerber et al (2009), and (d) Sun et al. (2009). It can be seen from Figure 5.11(a) that the simple linear compression is not sufficient for relief generation as many important features are missing. The others preserve more details, which can be applied to generating sunken reliefs by simply shifting the height into its surface. However, the results generated by this way are compromised and degenerated because the important feature lines with carved effects are missing which sunken reliefs mostly rely on. The proposed approach is the first time that sunken relief generation has been proposed whcih benefits from the application of contour lines that impresses the presence of 3D features and addresses more variations in the art forms. Such lines are organically integrated with the smooth surfaces.
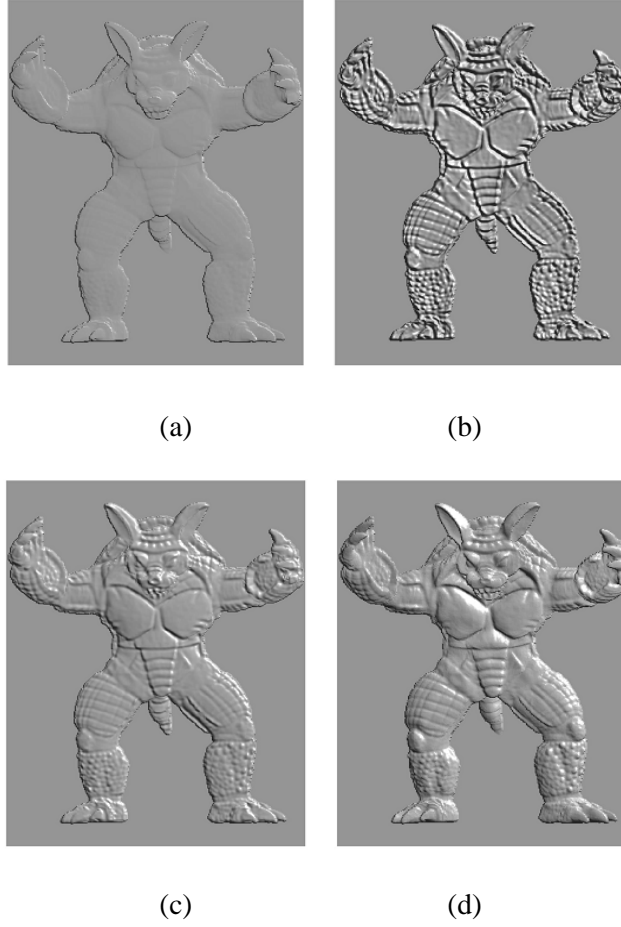
Figure 5. 11 Bas reliefs produced by the methods of (a) Cignoni et al. (1997). (b) Kerber et al. (2007). (c) Kerber (2009). (d) Sun et al. (2009).

Figure 5.12 shows multiple results created by using the proposed. It demonstrates that the proposed method is able to handle both simple abstraction forms (Figure 5.12(a), the Pear), and complex geometric features (Figure 5.12(d), the Buste). Very low frequency but smooth features like the muscles along the shoulders of the horse or the neck of the pear could hardly be preserved if only the height information is taken into account. The example of the Heptoroid shows that the depth order remains visible.

(a) Pear model.
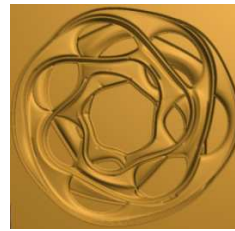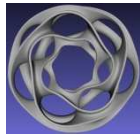
(b) Heptoroid.
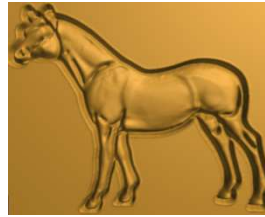
(c) Horse.

(d) Buste.

Figure 5. 12 The results of sunken reliefs.

In this experiment, different 3D meshes are used as inputs to create the sunken reliefs. The user is able to control the sunken relief outputs with different settings in preparing their inputs. The PC used is HP Workstation 4300, with

Intel Pentium Dual CPU 3.2GHz and 2GB RAM, which is equipped with NVIDIA GeForce 7900 GTX video card. It takes 6-20 seconds of processing time to create a relief from images with resolution of 1024x768. For example, the Cow model (Figure 5.9(c)) was created in 6.67 seconds and Armadillo model (Figure 5.10((a)) in 18.07 seconds. The variance of time depends on the resolution as well as the complexity of the reliefs. As the algorithm is implemented in Matlab, it would be foreseen an improvement of performance when rewriting the code in C++.

5.6 Summary

In this chapter, firstly, a technique to generate sunken relief has been proposed using lines extracted from line drawings. Following this, a novel combination a line drawing image with an image rendered using Lambertian shading and with a depth image has been developed. This combination of these three elements is able to generate more lively and vivid sunken reliefs. The experiments have shown that the former can generate sunken relief models with pure engraved lines, whilst the latter can generate smooth height information between lines. The combination of lines and height transition can effectively generate advanced sunken relief compared to the former one.

CHAPTER 6

CONCLUSIONS AND FUTURE WORK

6.1 Conclusions

This thesis has developed techniques for generating three types of relief (bas relief, high relief and sunken relief) digitally in a unified framework. These types of relief are distinguished with one another in terms of their definition and style, high relief has over half of their natural depth, bas relief has under half (a small value in most cases) of their natural depth and for sunken relief, the objects are carved into a flat surface (Rogers 1974).

My framework of digital relief generation includes: a novel bas relief generation method based on gradient operation from a single piece of image; an efficient method to generate a relief (both bas reliefs and high reliefs) from a 3D mesh directly; and the methods for sunken reliefs generated with only feature lines and with an improvement of combining feature/contour lines and

the depth information. These developed methods are related to one another although they are specially designed to solve different problems.

The methods are designed to consider various inputs, including images and 3D meshes. The relief generation from an image is the most simple and mature technique to create relief-style. It is only confined to generate bas reliefs and hard to extend to high relief generation. The relief generation from 3D shapes has been considered as a promising way to create both high relief and bas relief, and this method allows reusing of existing 3D models of different objects. The produced relief do convey height information and then can be machined into relief pieces with a CAM system. The development of these techniques is motivated by a systematic review of existing works in this field. The developed knowledge in this thesis can assist both relief artists (relief sculptors) and aesthetic designers to achieve a better understanding and develop a new viewpoint on relief production and its applications.

The developed bas relief generation method was based on gradient operation on a single image. Image gradient operation highly improves the quality of generated reliefs by enhancing and preserving the details. This method is able to generate bas relief models and provides true 3D information rather than a pseudo relief artwork as an image which contains "fake" depth information. My method can be adopted to use 3D models if the models can be converted into height fields discretized on a uniformed grid. Taking such height fields as a grey image input, the method can be directly applied to compressing the height into bas reliefs. This digitally generated bas relief bridges the gap between image processing tools and industrial design packages in that the generated reliefs contain height information as meshes and can be used as inputs for industrial design packages. However, like all other image-based reconstruction algorithms (Said et al. 2009), the proposed method is sensitive to colour distribution which may cause unnatural discontinuity in the results

when using a colour image as an input. It needs to introduce a way to authentically interpret a colour image into a gray image to allow my method working effectively. Another limitation of this method is that it is designed to create reliefs with shallow carving, thus it cannot be applied for high relief generation. Although works on SfS may be relevant to high relief generation, it would be beneficial to introduce a perception model and an intelligent algorithm to recognize shapes from images.

The problem of modelling high reliefs encodes more complex geometry and richer depth variance than bas reliefs. The proposed method to generate relief (both bas relief and high relief) is from a 3D mesh directly. This method applied 3D Unsharp Masking to boost the details of 3D objects. A non-linear scaling scheme was developed to achieve the designed effects in compression. The produced reliefs contain actual height information which can be used as inputs for a CAM system. The core technique of this method is the preservations of the details, while I used Laplacian smoothing to help extract out the details for 3D Unsharp masking. Other advanced mesh filters, such as bilateral filer, cross-bilateral filter etc. can be used to replace Laplacian smoothing to get non-linear features and thus benefit the relief modelling.

Two styles of sunken reliefs were generated, one used pure engraved lines to present the features/shapes, and the other combined the extracted feature lines with depth variation. The latter one can generate smooth height transition between lines to emphasize the perception of a 3D shape. This work is the first attempt to create sunken relief digitally. However, the created sunken reliefs used certain line types, including contours, ridges and creases, other stylization of secondary lines may be required to present certain effects, for example, to convey shape shadow with hatch lines, and the generation of these secondary lines is not included in my thesis so far. Although the proposed sunken relief generation method starts from a 3D mesh, the generation of the relief firstly

transforms mesh information into several image-like inputs, implying that image based bas relief generation method can be adopted here.

This thesis has proposed methods to generate bas reliefs, high reliefs and sunken reliefs, these methods are related to one another. For example, bas relief, high relief and sunken relief can be all generated from 3D inputs with developed methods. For bas relief and high relief generation, different Scaling Factor is required, and for sunken relief generation, the lines and shape information can be extracted from 3D models and then be combined. By converting 3D models into height field data, the gradient operation based method can be used to generate bas reliefs. This image based bas relief generation technique can also be directly adopted for sunken relief generation to achieve different results and stylizations if a line detection algorithm is included.

6.2 Future work

There are still some other aspects to be investigated in the future to extend this research, like stylization, animation and spatial arrangement of the generated reliefs.

Deformation can stylise the generated reliefs such as realistic relief, abstract relief and combination relief according to the definition. Geometric transformation methods (Alexa 2003; Sheffer and Kraevoy 2004; Jin et al. 2000; Jones et al. 2003) could be applied to developing the stylised reliefs achieving some special deformation effects. A wire based geometric deformation technique could be developed (Igarashi et al. 2007) to achieve different deformation effects as well.

Combining current animation techniques in producing relief-style animation offers a novel representation for games and movies. Developing techniques for relief-style animations (Moccozet et al. 2004; Baran et al. 2007) will be applicable for games or films. There are two possible ways to realise relief animation: The first one is converting existing 3D animation sequences to 3D relief animation directly; the other one is making relief animation from processing digital relief models by adopting deformation(Sumner and Popovi 2004) and morphing techniques(Fidaleo et al. 2000).

Improving previously developed techniques will solve some specific problems relating to real relief production, such as overlapping, foreshortening, colouring and lighting. Relief is a spatial art form (Rogers 1974). What should be considered next is to solve the overlapping problem when there is more than one object in a scene because the overlapping of shapes serves a variety of decorative and expressive purposes. For computer realization, the most obvious and straightforward method of overlapping a number of forms in a limited space is to put all the forms into different planes of relief, so that the foremost layer constitutes the front plane and the other layers lie in a series of receding planes between this front plane and the background. Another choice is to carve the more advanced figures in high relief and the deeper-lying figures in low relief and keep them both in separate planes. Foreshortening occurs when an object appears compressed when observed from a peculiar viewpoint, and the effect of perspective causes distortion. It is a familiar pictorial method of representing the recession of objects. A simple and well known instance is the use of an ellipse to represent a receding circle. Another way of avoiding extreme foreshortening while also avoiding the extreme loss of depth is arranging everything parallel with the picture plane.

References:

Agrawal, A., Raskar, R. and Chellappa, R., 2006. "What is the Range of Surface Reconstructions from a Gradient Field?". *European Conference on Computer Vision*.

Aim Shape, 2009. *3D models*. Available from:
http://shapes.aim-at-shape.net/viewmodels.php [Access 28 August 2009].

Alexa, M., 2003. Differential coordinates for local mesh morphing and deformation. *The Visual Computer,* 19(2), 105-114.

Alexa, M., 2005. Mesh Editing based on Discrete Laplace and Poisson Models. *In Eurographics Tutorial 5 - Interactive Shape Modelling*.

Alexa, M. and Matusik, W., 2010. Reliefs as images. *ACM Transactions on Graphics*, 29(4), 1-7.

ArtCAM, 2009. *Relief producing software*. Available from:
http://www.artcam.com [Accessed 25 August 2009].

Artist Unknown, 1336 BC. *Akhenaten, Painted limestone (sunken relief)*. Egypt.
http://cdn.wn.com/pd/12/26/13a51c42ae698e9b969138c74353_grande.jpg[Accessed 25 March 2011].

Badamchizadeh, M.A. and Aghagolzadeh, A., 2004. Comparative study of unsharp masking methods for image enhancement. *In International Conference on Image and Graphics*, 27-30.

Baran, I. and Popovic, J., 2007. Penalty functions for automatic rigging and animation of 3D characters. *Proceedings of the 2007 SIGGRAPH Conference*, 26(3).

BattlestarVII, 2011. *A wooden statue of the Buddha*. Museum of Shanghai. Available from:

http://commons.wikimedia.org/wiki/File:Wooden_buddha_statue.jpg.
[Accessed 02 March 2011].

Belhumeur, P.N., Kriegman, D.J. and Yuille, A.L., 1999. The bas-relief ambiguity. *International Journal of Computer Vision*, 35(1), 33-44.

Blinn, J.F., 1978. Simulation of Wrinkled Surfaces. *ACM SIGGRAPH Computer Graphics,* 13(2), 86-292.

British Museum, 2009a. *The Parthenon Sculptures*. Available from:

http://www.britishmuseum.org/research [Accessed 02 December 2009].

British Museum, 2009b. *The Coffin*. Available from:

http://www.britishmuseum.org/research/ [Accessed 02 December 2009].

Causey, A., 1998. *Sculpture since 1945*. Oxford University Press, USA.

China Visual, 2009. *2D relief animation*. Available from:
http://static.chinavisual.com/storage/resources/2007/04/17/133519I178938P34
782T1.jpg.shtml [Accessed 28 August 2009].

Cignoni, P., Montani, C. and Scopigno, R., 1997. Computer-assisted generation of bas- and high- reliefs. *Journal of Graphics Tools*, 2 (3), 15-28.

Cignoni, P., Montani, C. and Scopigno, R., 1998. A Comparison of Mesh Simplification Algorithms, *In Computers & Graphics*, 22(1), 37-54.

Cignoni, P., Scopigno, R. and Tarini, M., 2005. A simple normal enhancement technique for interactive non-photorealistic renderings. *Computer & Graphics, 29*(1), 125-133.

Cole, F., Golovinskiy, A., Limpaecher, A., Barros, H.S., Finkelstein, A., Funkhouser, T. and Rusinkiewicz, S., 2008. Where do people draw lines? *ACM Transactions on Graphics*, 27(3), 1-11.

Cole, F., Sanik, K., Decarlo, D., Finkelstein, A., Funkhouser, T., Rusinkiewicz, S. and Singh, M., 2009. How well do line drawings depict shape? *ACM Transactions on Graphics,* 28(3), 1-9.

Decarlo, D., Finkelstein, A. and Rusinkiewicz, S., 2004. Interactive rendering of suggestive contours with temporal coherence. *In Proceedings of the 3rd International Symposium on Non-photorealistic Animation and Rendering*, 15-145.

Decarlo, D., Finkelstein, A., Rusinkiewicz, S. and Santella, A., 2003. Suggestive contours for conveying shape. *ACM Transactions on Graphics*, 22(3), 848–855.

Desbrun, M., Meyer, M. Schrder, P. and Barr, A.H., 1999. Implicit fairing of arbitrary meshes using diffusion and curvature flow. *Proceedings of the 26th Annual Conference on Computer Graphics and Interactive Techniques*, 317-324.

Durand, F. and Dorsey, J., 2002. Fast bilateral filtering for the display of high-dynamic-range images. *ACM Transactions on Graphics*, 21(3), 257-266.

Donnelly, W., 2005. Per-pixel displacement mapping with distance functions. *GPU Gems*, 2(2), 123-136.

Exchange3D, 2009. *Lion relief model*. Available from: http://www.exchange3d.com/cubecart/miscelaneous/lion-relief-2-3d-model/prod_3416.html [Accessed 23 August 2009].

Fattal, R., Lischinski, D. and Werman, M., 2002. Gradient domain high dynamic range compression. *ACM Transactions on Graphics*, 21(3), 249-256.

Fidaleo, D., Noh, J., Kim, T., Enciso, R. and Neumann, U., 2000. Classification and volume morphing for performance-driven facial animation. *International Workshop on Digital and Computational Video*.

Field, D.A., 1988. Laplacian smoothing and Delaunay triangulations. *Communications in Applied Numerical Methods*, 4(6), 709-712.

Flash, 2009. *Relief animation production*. Available from: http://www.adobe.com/products/flash/ [Accessed 25 August 2009].

Flaxman, J., 1829. *Lectures on sculpture*. Charles Knight, Pall Mall East, London.

Floater, M.S., 2003. Mean value coordinates. *Computer Aided Geometric Design*, 20(1), 19-27.

FreeSpace, 2009. *Bump mapping*. Available from: http://freespace.virgin.net/hugo.elias/graphics/x_polybm.htm [Accessed 1 September 2009].

Gabriel, P., 2009. *Toolbox graph*. Available from: http://www.ceremade.dauphine.fr/~peyre/matlab/graph/content.html [Accessed 20 October 2009].

Gorbis Images, 2009. *Temple of Ramesses II in Abu Simbel: Sunk-relief of Captives of the Asiatic War on the Entrance Walls.* Available from: http://www.corbisimages.com/Enlargement/Enlargement.aspx?id=VN003455 &ext=1[Accessed 02 December 2009].

Hansen, G.A., Douglass, R.W. and Zardecki, A., 2005. *Mesh enhancement*. Imperial College Press.

Haralick, R.M. and Shapiro, L.G., 1992. *Computer and robot vision*. Addison-Wesley Longman Publishing Co., Inc. Boston, MA, USA.

Heckbert, P.S., 1986. Survey of Texture Mapping. *IEEE Computer Graphics and Applications*, 6(11), 56-67.

Hirche, J., Ehlert, A., Guthe, S. and Doggett, M., 2004. Hardware accelerated per-pixel displacement mapping. *Proceedings of Graphics Interface*, 153-158.

Horn, B. and Brooks, M., 1986. The variational approach to shape from shading. *In Computer Vision, Graphics and Image Processing*, 33,174-208.

Igarashi, T., Matsuoka, S. and Tanaka, H., 2007. Teddy: a sketching interface for 3D freeform design. *ACM SIGGRAPH 2007 courses*.

Ihrkea, M., Ritschelc, T., Smithc, K., Groschc, T., Myszkowskic, K. and Seidelc, H.P., 2009. A perceptual evaluation of 3D unsharp masking. *Society of Photo-Optical Instrumentation Engineers Conference Series*.

Isenburg, M., Lindstrom, P., Gumhold, S. and Snoeyink, J., 2003. Large Mesh Simplification using Processing Sequences. *Proceedings of Visualization'03*, 465-472.

Jin, X., Li, Y.F. and Peng, Q., 2000. General constrained deformations based on generalized metaballs. *Computers & Graphics*, 24(2), 219-231.

Jones, T.R., Durand, F. and Desbrun, M., 2003. Non-iterative, feature-preserving mesh smoothing. *ACM Transactions on Graphics*. 22(3), 943-949.

JustEasy. *Sphinx*, 2009. Available from:
http://www.justeasy.cn/buydownload.asp?id=5742 [Accessed 20 June 2009].

Kalnins, R.D., Markosian, L., Meier, B.J., Kowalski, M.A., Lee, J.C., Davidson, P.L., Webb, M., Hughes, J.F. and Finkelstein, A., 2002. WYSIWYG NPR: drawing strokes directly on 3D models. *ACM Transactions on Graphics*. 21(3), 755-762.

Keith, W., 2009. *How Unsharp Masking and Laplacian Sharpening Work*. Available from:
http://keithwiley.com/astroPhotography/imageSharpening.shtml [Accessed 25 September 2009].

Kerber, J., 2007. "Digital Art of Bas-Relief Sculpting," *Master's thesis*, Univ. of Saarland, Saarbrü cken, Germany.

Kerber, J., Belyaev, A. and Seidel, H.P., 2007. Feature preserving depth compression of range images. *Proceedings of the 23rd Spring Conference on Computer Graphics*, 110-114.

Kerber, J., Tevs, A., Belyaev, A., Zayer, R. and Seidel, H.P., 2009. Feature Sensitive Bas Relief Generation. *IEEE International Conference on Shape Modelling and Applications*, 148-154.

Kerber J., Tevs A., Zayer R., Belyaev A. and Seidel P., 2010. Real-time generation of digital bas-reliefs. *Computer-Aided Design and Applications, Special Issue: CAD in the Arts*, 7(4), 465-478.

Kim, M.H. and MacDonald, L.W., 2006. Rendering high dynamic range images. *In Proceedings of 17th Anuual Electronic Media & Visual Arts Conference 2006*, 1-10.

Koenderink, J.J., 1984. What does the occluding contour tell us about solid shape? *Perception*, 13(3), 321-330.

Lee, C.H., Varshney, A. and Jacobs, D.W., 2005. Mesh saliency. *ACM SIGGRAPH 2005 Papers*, 659-666.

Luft, T., Colditz, C. and Deussen, O., 2006. Image enhancement by unsharp masking the depth buffer. *ACM Transactions on Graphics*. 25(3), 1206-1213.

Maini, R. and Aggarwal, H., 2009. Study and Comparison of Various Image Edge Detection Techniques. *International Journal of Image Processing,* 3(1), 1-11.

Markosian, L., Kowalski, M.A, Goldstein, D., Trychin, S.J., Hughes, J.F. and Bourdev L.D., 1997. Real-time nonphotorealistic rendering. *In SIGGRAPH'97*, 415-420.

Mathieu, D., Mark, M., Peter, S., and Alan H.B., 1999. Implicit fairing of irregular meshes using diffusion and curvature flow. *In SIGGRAPH '99:*

Proceedings of the 26th Annual Conference on Computer Graphics and Interactive Techniques, 317-324.

Moccozet, L., Dellas, F., Magnenat-thalmann, N., Biasotti,S., Mortara, M., Falcidieno, B., Min, P. and Veltkamp, R., 2004. Animatable human body model reconstruction from 3D scan data using templates. *In Captech Workshop on Modelling and Motion Capture Techniques for Virtual Environments*, 73-79.

Nicknorris, 2009. *Stone Sculpture.* Available from: http://www.nicknorris.com/stone_carving_process.htm [Accessed 26 February 2009].

Orzan, A., Bousseau, A., Winnem¨oller, H., Barla, P., Thollot, J. and Salesin, D., Diffusion curves: a vector representation for smooth-shaded images. *ACM SIGGRAPH 2008 papers*, 1-8.

Owen, S.J., 1998. A survey of unstructured mesh generation technology. *The 7th International Meshing Roundtable*, 3(6).

Paris, S. and Durand, F., 2006. A fast approximation of the bilateral filter using a signal processing approach. *In Proceedings of the European Conference on Computer Vision*, 568-580.

Peercy, M., Airey, A. and Cabral, B., 1997. Efficient Bump Mapping Hardware. *In proceedings of SIGGRAPH 97*, 303-306.

P´erez, P., Gangnet, M. and Blake, A., 2003. Poisson image editing. *ACM Transactions on Graphics*, 22(3), 313-318.

Perry, R.N. and Frisken, S.F., 2001. Kizamu: a system for sculpting digital characters. *In ACM Transactions on Graphics*, 47-56.

Photoshop, 2009. *Relief filter*. Available from: https://www.photoshop.com/ [Accessed 25 August 2009].

Prados, E. and Faugeras, O., 2005. Shape from shading: A well-posed problem? *IEEE Computer Society*.

Pudn, 2009. *Bump mapping*. Available from: http://www.pudn.com/detail.asp?id=471459 [Accessed 25 August 2009].

Raskar, R., 2001. Hardware support for non-photorealistic rendering. *Proceedings of the ACM SIGGRAPH/EUROGRAPHICS Workshop on Graphics Hardware*, 41-47.

Ritschel, T., Smith, K., Ihrkea, M. ,Grosch, T., Myszkowski, K. and Seidel, H.P., 2008. 3D unsharp masking for scene coherent enhancement. *ACM Transactions on Graphics*, 7(3), 1-8.

Rogers, L.R., 1974. *Relief sculpture*. Oxford University Press, Oxford.

Rogers, D.F. and Earnshaw, R.A., 1990. Computer Graphics Techniques: theory and practice. *Springer*.

Rusinkiewicz, S., Cole, F., Decarlo D. and Finkelstein, A., 2008. Line drawings from 3D models. *SIGGRAPH 2008 Course Notes*, 1-356.

Said, M., Hasbullah, H. and Baharudin, B., 2009. Image-based modelling: a review. *Journal of Theoretical Applied Information Technology*, 5(2), 200-215.

Sheffer, A. and Kraevoy, V., 2004. Pyramid coordinates for morphing and deformation. *IEEE Computer Society*.

Smith, C., 2006. *On vertex-vertex systems and their use in geometric and biological modelling*. Thesis, (PhD). University of Calgary.

Song, W., Belyaev, A. and Seidel, H.P., 2007. Automatic generation of bas-reliefs from 3D shapes. *Proceedings of the IEEE International Conference on Shape Modelling and Applications*, 211-214.

Sorkine, O., Cohen-Or, D., Lipman, Y., Alexa, M., Rossl, C. and Seidel, H.P., 2004. Laplacian surface editing. *Proceedings of the 2004 Eurographics/ACM SIGGRAPH Symposium on Geometry Processing*, 175-184.

Sourin, A., 2001a. Functionally based virtual computer art. *In SI3D '01: Proceedings of the 2001 Symposium on Interactive 3D Graphics*, 77-84.

Sourin, A., 2001b. Functionally based virtual embossing. *The Visual Computer, Springer,* 17(4), 258–271.

Sousa, M.C. and Prusinkiewicz, P., 2003. A few good lines: Suggestive drawing of 3d models. *Computer Graphics Forum*, 22(3), 381-390.

Sumner, R.W. and Popovi J., 2004. Deformation transfer for triangle meshes. *ACM SIGGRAPH 2004*, 23(3), 399-405.

Sun, X., Rosin, P.L., Martin, R.R. and Langbein, F.C., 2009. Bas-relief generation using adaptive histogram equalization. *IEEE Transactions on Visualization and Computer Graph*ics, 15(4), 642-653.

Takayama, N., Meng, S. and Hiroki, T., 2010. Choshi design system from 2D images. *International Conference on Entertainment Computing*, 358-365.

Tobler, R.F. and Maierhofer, S., 2006. A Mesh Data Structure for Rendering and Subdivision. *in Proceedings of International Conference in Central Europe on Computer Graphics, Visualization and Computer Vision*, 157-162.

Vollmer, J., Mencl, R. and Mueller, H., 1999. Improved Laplacian smoothing of noisy surface meshes. *Computer Graphics Forum*, 18(3), 131-138.

Wang, X., Tong, X., Lin, S., Hu, S., Guo, B. and Shum, H.Y., 2004. Generalized displacement maps. *Eurographics Symposium on Rendering*, 227-233.

Weiss, B., 2006. Fast median and bilateral filtering. *ACM Transactions on Graphics,* 25(3), 519-526.

Weyrich, T. Deng, J., Barnes, C., Rusinkiewicz, S. and Finkelstein A., 2007. Digital bas-relief from 3D scenes. *ACM Transactions on Graphics*, 26(3), 32-39.

Wu, T.P., Sun, J., Tang, C.K. and Shum, H.Y., 2008. Interactive Normal Reconstruction from a Single Image. *ACM Transactions on Graphics*, 27(5), 1-9.

Zeng, G., Matsushita, Y., Quan, L. and Shum, H., 2005. Interactive shape from shading. *IEEE Computer Society*, 343-350.

Zhang, R., Tsai, P, Cryer, J. E., and Shah, M., 1999. Shape from Shading: A Survey. *IEEE Transactions on Pattern Analysis and Machine Intelligence*, 21(8), 690-706.